Master Thesis, Department of Geosciences

Palynology and Sedimentology of the Dunscombe Formation, Mercia Mudstone Group, South Devon, Southwest England

Ilias Kousis

Supervisors:
W. M. Kuerschner
S. Mueller

UNIVERSITY OF OSLO
FACULTY OF MATHEMATICS AND NATURAL SCIENCES

Palynology and Sedimentology of the Dunscombe Formation, Mercia Mudstone Group, South Devon, Southwest England

August 2015

Ilias Kousis

Master Thesis in Geosciences

Discipline: Palynology/Sedimentology

Department of Geosciences

Faculty of Mathematics and Natural Sciences

University of Oslo

August 2015

Acknowledgements

I would first like to thank my main supervisor Wolfram Kuerschner for his trust and valuable guidance throughout the project as well as Steven Mueller for his feedback, corrections and all the skills he taught me. I am grateful to Viktoria Baranyi who pushed me to my limits and aided me a great deal on the palynological part. I wish to thank Ramues Gallois and Mark Hounslow, who contributed in my fieldwork and provided me with additional material to study and use for the research of this work. I sincerely thank Maarten Aerts for his guidance on the X-ray diffraction method and for the fruitful discussions. I thank Berit Løken Berg for her initial assistance in the lab. I am thankful to Johan Petter Nystuen for the discussions on the mineralogy. Last but not least, I am very grateful to my family for both their financial and mental support as well as my friends; for it would be impossible to carry out this project without their support. Thank you very much all of you.

Table of Contents

Abstract

The Late Triassic in Europe has been suggested to represent a period of stable dry continental climate interrupted in the Julian (Carnian) by a distinct humid pulse that shows a pluvial character. The effects of this short-lived and possibly even, global climatic event, are recorded both in the sedimentological and palynological aspects of the rock formations. The humidification of the climate in the case of Dunscombe Formation, in South Devon, Southwest England, is proved by the palynofacies trends, the presence of algae remains as well as by the mineralogical components (increase of kaolinite) and by optical microscopy of thin sections. The presence of ooids in thin sections implies the existence of a lake of considerable size strengthened at the same time by the presence of the fresh-water algae, *Plaesiodictyon*. The study concludes that indeed the lithology, the palynofacies and palynology seem to be linked predominantly with the climatic variations and secondarily with the tectonic activity and the palaeogeography.

1. Introduction

1.1. Scientific rationale: Palaeoclimate in Late Triassic

The palaeoclimate of the Triassic was initially considered to be predominantly arid (e.g. Retallack et al., 1996) and stable (e.g. Hallam, 1985; Dickins, 1993). However, recent studies began to show that in addition to the arid background, it was also characterized by seasonality and alternations between arid and humid periods (e.g. Simms and Ruffell, 1989; Ruffell and Hounslow, 2006; Preto et al., 2010; Haas et al., 2012). Evidence for presence of polar ice caps in the sedimentary record during the Triassic is lacking (Ruffell and Hounslow, 2006). Many authors have presented evidence of sediments having been deposited under wet conditions (e.g. Simms and Ruffell, 1989; Gallois and Porter, 2006; Porter and Gallois, 2008; Hochuli and Vigran, 2010; Kolar-Jurkovšek and Jurkovšek, 2010; Kozur and Bachmann, 2010; Rostási et al., 2011).

Several publications suggest a shift towards a wetter climate in locations of Western Tethys during the Late Triassic (e.g. Simms and Ruffell, 1989; Hornung and Brandner, 2005; Rigo et al., 2007; McKie and Williams, 2009; Kozur and Bachmann, 2010; Preto et al., 2010; Roghi et al., 2010; Arche and López-Gómez, 2014; Dal Corso et al., 2015), which are relevant to the present study location.

Hornung and Bradner (2005) and Hornung et al. (2007a and b) reported a shift towards a climate with higher precipitation rates as implied by the demise of carbonate platforms and their interruption by clastic sediments.

Kozur & Bachmann (2010) referred to a “Mid Carnian Wet Intermezzo” in Germany expressed by a siliciclastic interval, the Schilfsandstein. Moreover, the authors concluded that this interval is contemporaneous with other similar deposits in northwestern Tethys and it was climatically induced (due to megamonsoonal circulation). They estimated the duration of this wet interval to be between 0.7–0.8 Ma. Interestingly, Gallois & Porter (2006) believe that the Dunscombe Mudstone Formation is represented by a condensed interval occupying the Carnian stage (~11.5 Ma) based on palaeomagnetic and palynological data. Their studied succession (35–40 m) is the study topic of the present study as well (same interval and location, different outcrops).

Kolar-Jurkovsek and Jurkovsek (2010) described a hygrophytic palynomorph assemblage in clastic horizons within a Carnian carbonate sequence in Slovenia. In Hungary Rostasi et al. (2011) and Haas et al. (2012) utilized clay mineralogy to define the Julian as a wet period. According to them, it is indicated by the abundance of illite, chlorite and IS (Illite-Smectite ratio) associated with kaolinite.

Preto et al. (2010) suggested that the Carnian is expressing the peak of monsoonal activity during the Triassic and after that the climate shows a more stable pattern. The monsoonal climatic pattern that is believed to have prevailed in Carnian might be linked with the flood basalts eruption (Wrangellia LIP) in western North America (as implied by Dal Corso et al., 2012; Ogg, 2015). However, this volcanic event was proved to have been already active prior to this change towards a more humid climate (Dal Corso et al., 2015; Mueller et al., 2015 and references therein). Dal Corso et al. (2015) suggested that “the injection of ^{13}C-depleted CO_2 into the Carnian atmosphere-ocean system may have been directly responsible for the increase in rainfall by intensifying the Pangaean mega-monsoon activity”. Similarly, Ogg (2015) agrees on the same cause for increased precipitation in Carnian.

Furthermore, studies in England have also concluded deposition under wetter settings (Simms and Ruffell, 1989; Gallois and Porter, 2006; Porter and Gallois, 2008). Fisher (1985) refers to a turnover in palynoflora in South Devon and addresses the climate as a potential cause rather than a shift in local parameters. A different view, however, considers local parameters (extensive river system similar to that of Nile nowadays) as the dominant cause for a major palynofloral change instead of being a climatically induced result (Visscher et al., 1994). In this study, I will consider this climatic change a global event as mentioned by recent studies (e.g. Simms and Ruffell, 1989; Roghi et al., 2010). This event has been studied and referred to under various names such as ‘Carnian Pluvial Event’ or CPE (e.g. Simms and Ruffell, 1989; Hornung et al., 2007a; Hornung et al., 2007b), “Mid Carnian Wet Intermezzo” (Kozur and Bachmann, 2010), Carnian Pluvial Phase or CPP (Mueller et al., 2015). The arguments usually lie in the intensity and duration of the event among the different localities.

The Late Triassic, however, is a period also marked by environmental changes and is well known for the end-Triassic mass extinctions (Bonis et al., 2010 and references therein). Based on the information above it can be assumed that the Triassic is not, after all, a monotonous arid period as previously thought. However, the complexities are many and even though there have been many attempts to solve them, most of them still remain controversial.

1. 2. The working area

The terrestrial/lacustrine Dunscombe Mudstone Formation and especially the Carnian section in South Devon of around 35-40 m (depending on the exact outcrop) has been subject of studies for many years applying numerous palynological and sedimentological techniques (e.g. Fisher, 1972; Jeans, 1978; Fisher, 1982; Gallois, 2001; Gallois and Porter, 2006; Porter and Gallois, 2008). It is therefore important to comprehend and gain better control on the chronology of the section, the condensed (or not) intervals and how the lithological changes connect (or not) with the climatic shifts or other factors such as tectonics and palaeomorphology and find out which prevails over. Finally, it is important to be able to trace any climatic signals and find out if it is possible to connect them with the pluvial climatic event known as Carnian Pluvial Event (the name varies among the authors and various localities).

1.3. Statement of the problem and the aim of the study

The majority of the studies on this climatic event have shown more convincing results on marine rather than on terrestrial/lacustrine sediments. Very few studies have managed to document distinct variations in the climate during the Carnian either due to the low preservation potential or the lack of exposed outcrops. These challenges make this study important. The aim of this study is to provide useful information on the palaeoclimate and depositional environments from the Carnian interval of the Dunscombe Formation in South Devon, Southwest England.

1.4. Summary of the applied methods

In the present study both palynological and sedimentological methods have been applied. A palynofacies analysis (relative abundances, ternary plot) and a palynological analysis on pollen/spores and fresh-water algae were carried out for the palynological part. A mineralogical analysis based on X-ray diffraction bulks as well as their clay fraction (<2 μm) and an optical microscopy analysis on thin sections, were applied for the sedimentological part. The reason for combining palynological with sedimentological methods was that palynology by itself had not provided concrete results so far in the study area in any of the previous works in terms of chronology and depositional environments. Therefore, the sedimentological methods were utilized as supplementary to the palynology (mainly to palynofacies analysis) in order to provide a more detailed approach for the palaeoclimate and depositional environment settings.

2. Geological setting

2.1 Palaeogeography

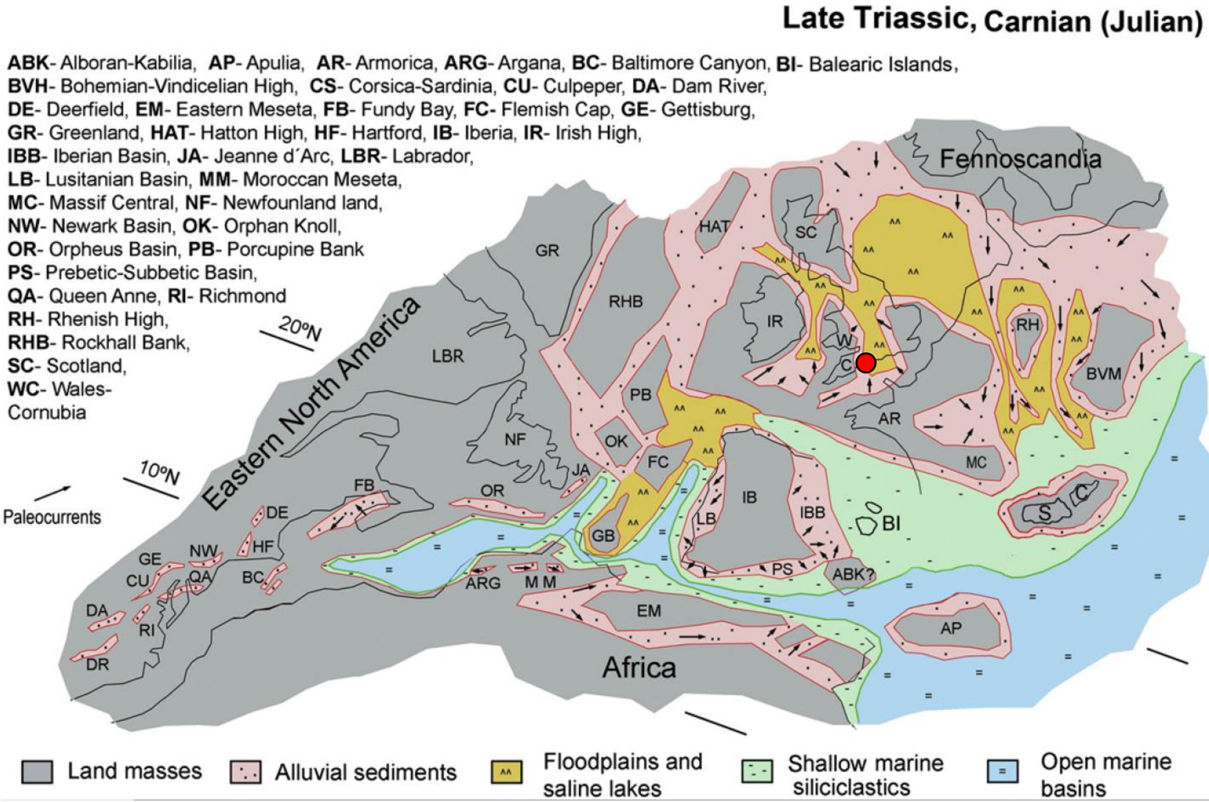

Figure 1: Palaeogeographic map of central eastern Pangea during Julian. Study area pinpointed by the red dot (modified from Arche and López-Gómez, 2014).

During the time of the Triassic, England was located in the interior of Pangaea, beyond the western termination of the Tethys Ocean. The Tethys Ocean had already been in the early stages of breaking apart. Therefore, in Europe this resulted in the formation of extensional, rift basins spreading from the Boreal Ocean, through Greenland – Norwegian rift passage into regions around Britain and also extended southwards into France, Iberia and central Europe (Ruffell and Hounslow, 2006, fig. 1). These basins were infilled with mostly fluvial sediments with thicknesses up to 8 km (Doré, 1992; McKie and Williams, 2009). The deposition of these alluvial facies was influenced by a number of factors such as variable subsidence, climate, sediment supply and marine influence (McKie and Williams, 2009).

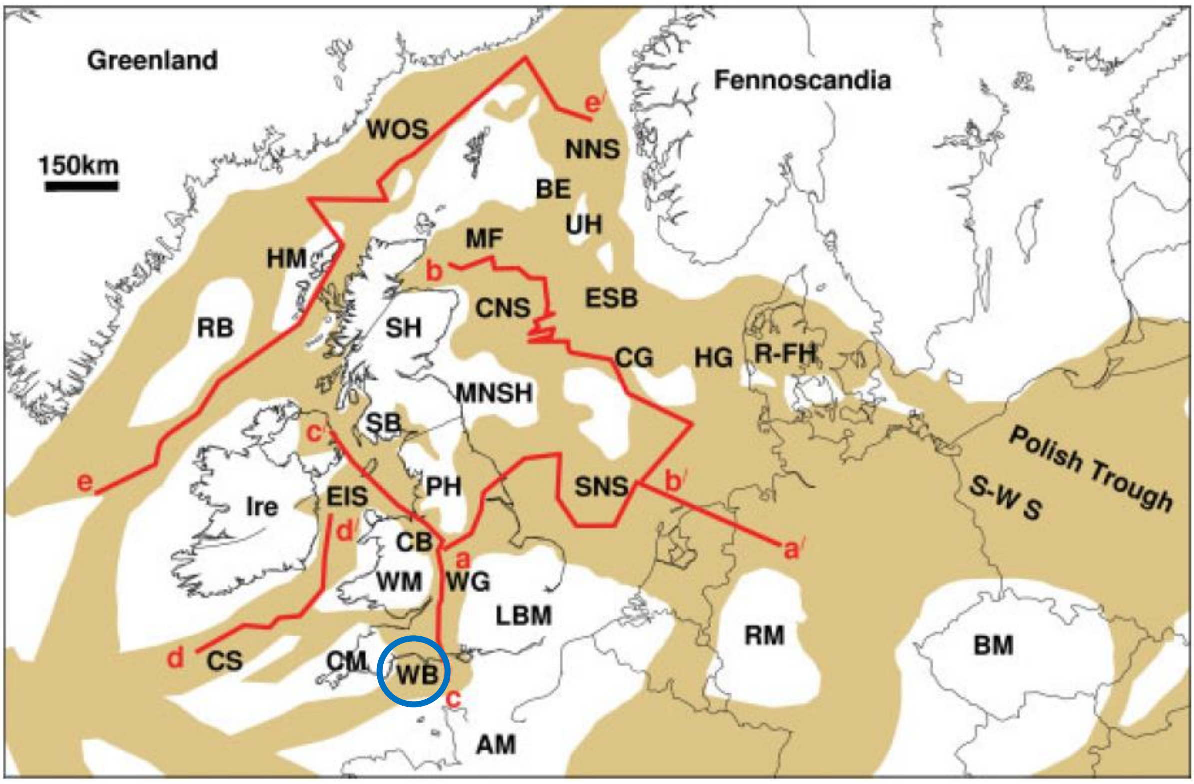

Figure 2: Triassic basins (brown), massifs and intrabasinal highs (white) in NW Europe. AM, Armorican Massif; BE, Beryl Embayment; BM, Bohemian Massif; CB, Cheshire Basin; CG, Central Graben; CM, Cornubian Massif; CNS, Central North Sea; CS, Celtic Sea; EIS, East Irish Sea; ESB, Eggersund sub-basin; HG, Horn Graben; HM, Hebrides Massif; Ire, Ireland; LBM, London-Brabant Massif; MF, Moray Firth; MNSH, Mid North Sea High; NNS, Northern North Sea; PH, Pennine High; R-FH, Ringkøbing–Fynn High; RB, Rockall Bank; RM, Rhenish Massif; SB, Solway Basin; SH, Scottish Highlands; SNS, Southern North Sea; S-WS, Szczecin-Wolsztyn Swell; UH, Utsira High; WB, Wessex Basin; WG, Worcester Graben; WM, Welsh Massif; WOS, West of Shetland. Our study area is in Wessex Basin marked by the blue circle (modified from McKie and Williams, 2009)

2.2. Outcrop locations and position of the samples

The Mercia Mudstone Group was deposited between the Middle to Late Triassic and is extensively exposed in the cliffs on the East Devon coast. The first outcrop is located on the Lower Dunscombe Cliff between Hook Ebb and Weston Mouth and the second on the Weston Cliff slightly east of Weston Ebb (Figs. 3-5).

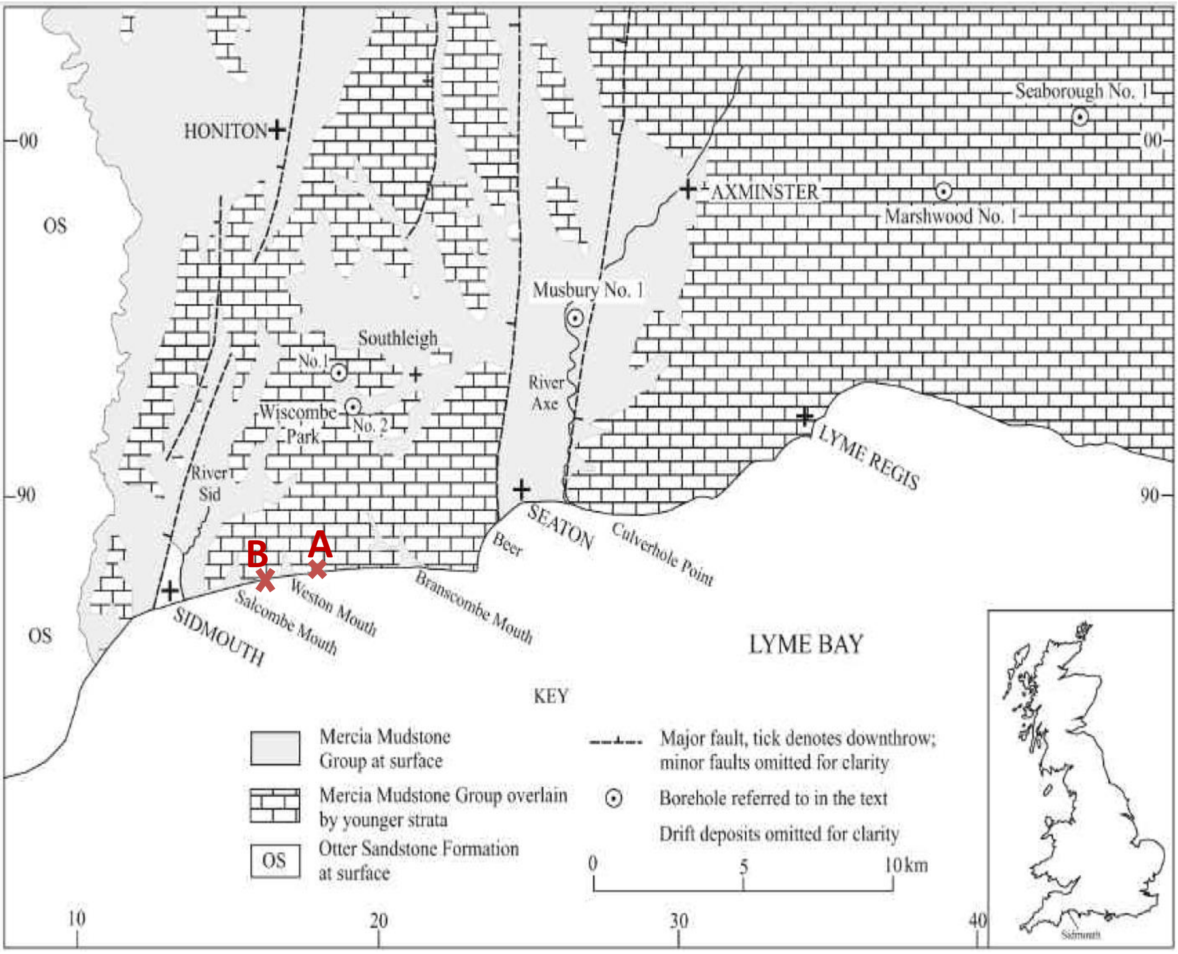

Figure 3: Geological sketch map of the study area showing the study outcrops of the Mercia Mudstone Group in SE Devon. The study outcrops are marked with red crosses A and B (modified from Gallois, 2007).

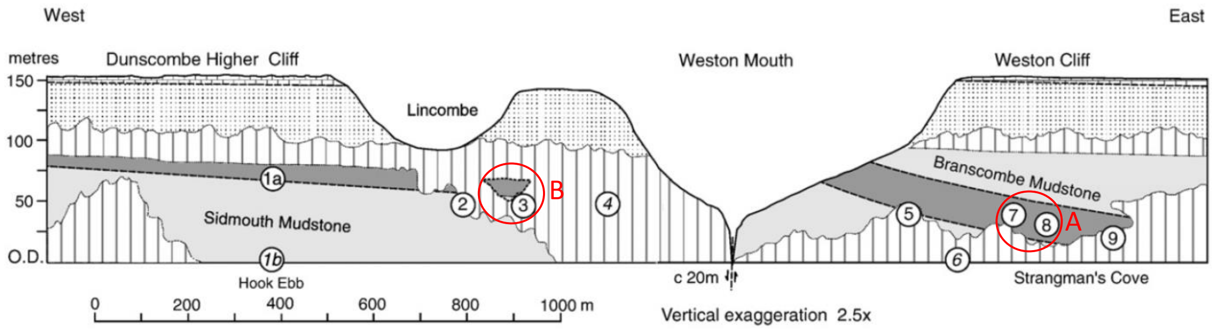

Figure 4: Sampling locations A and B on outcrop (modified from Porter and Gallois, 2008).

Figure 5: Location of the outcrops from Google Earth

Figure 6: Sampling outcrop A

Figure 7: Sampling outcrop B

Figure 8: Sampling outcrop A

2.3. Sedimentology

The Mercia Mudstone Group consists of approximately 450 m of red mudstones and associated evaporates and is considered to be the British equivalent of Keuper Marl facies in NW, like the Schilfsandstein in the Germanic Basin (e.g. Jeans, 1978; Howard et al., 2008; Porter and Gallois, 2008). The present study focuses on the middle part of the Group which has been assigned with a Carnian age (Gallois and Porter, 2006) that might extends up to Norian in the upper part (personal communication with Mr. Hounslow). Emphasis will be up on the Carnian interval represented by the Arden Sandstone Formation (Howard et al., 2008), which is an alternative name for Dunscombe Mudstone Formation. On the Devon coast this consists of a 35–40 m thick section of green, purple and grey laminated mudstones interbedded with calcareous siltstones/sandstones and breccias (e.g. Gallois, 2001; Porter and Gallois, 2008). This interval is known to vary laterally, which was confirmed by field observations during the fieldwork of this study.

The stratigraphical description following was based on field observations and correlates with the descriptions provided by Howard et al. (2008) mentioned as Arden Sandstone Formation and Porter and Gallois (2008) mentioned as Dunscombe Mudstone Formation, including the Lincombe Member.

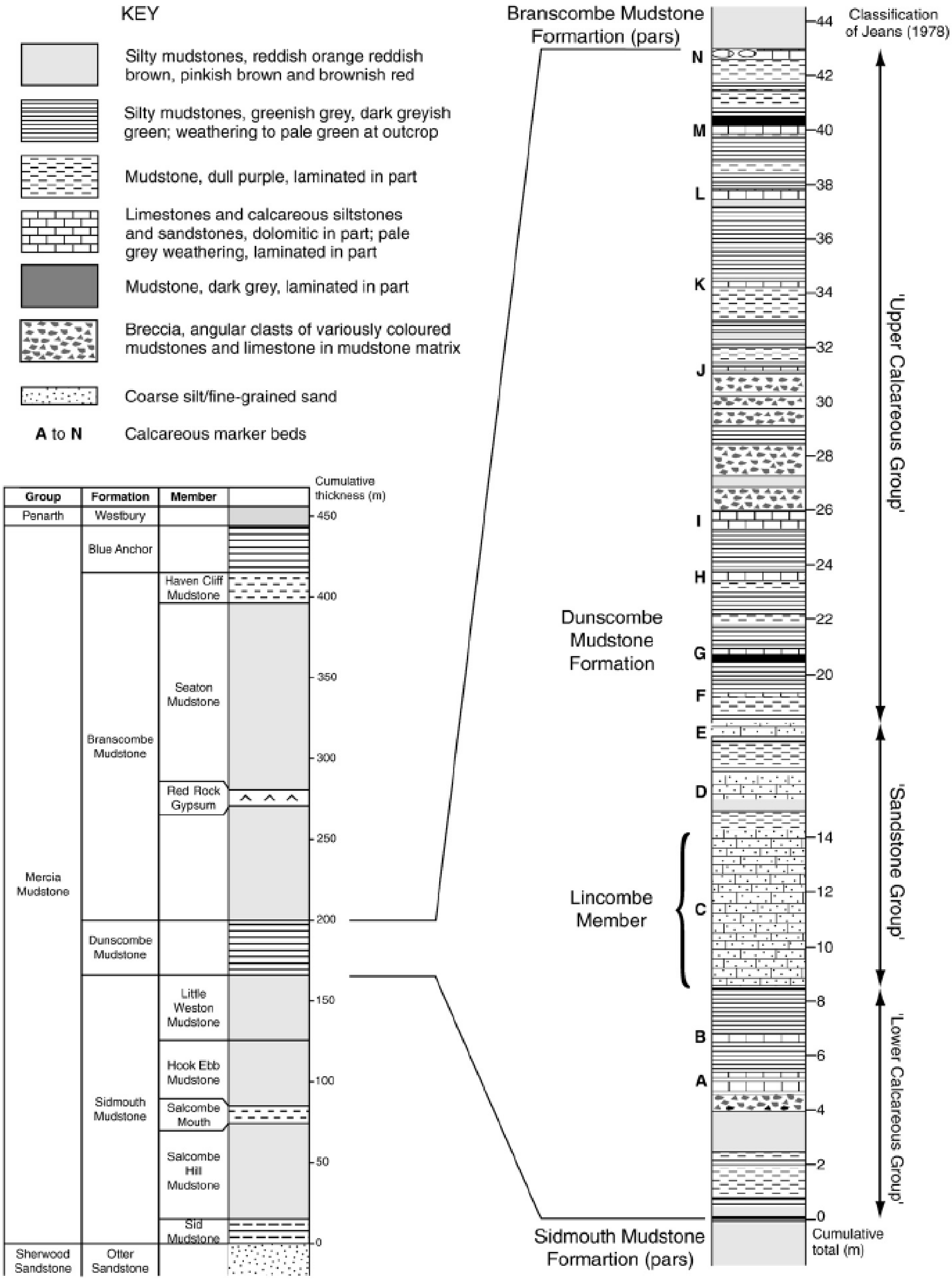

Figure 9: Lithological subdivision of Dunscombe Mudstone Formation from Porter and Gallois, 2008. The subdivision according to Jeans, 1978 is also presented on the right of the lithological column.

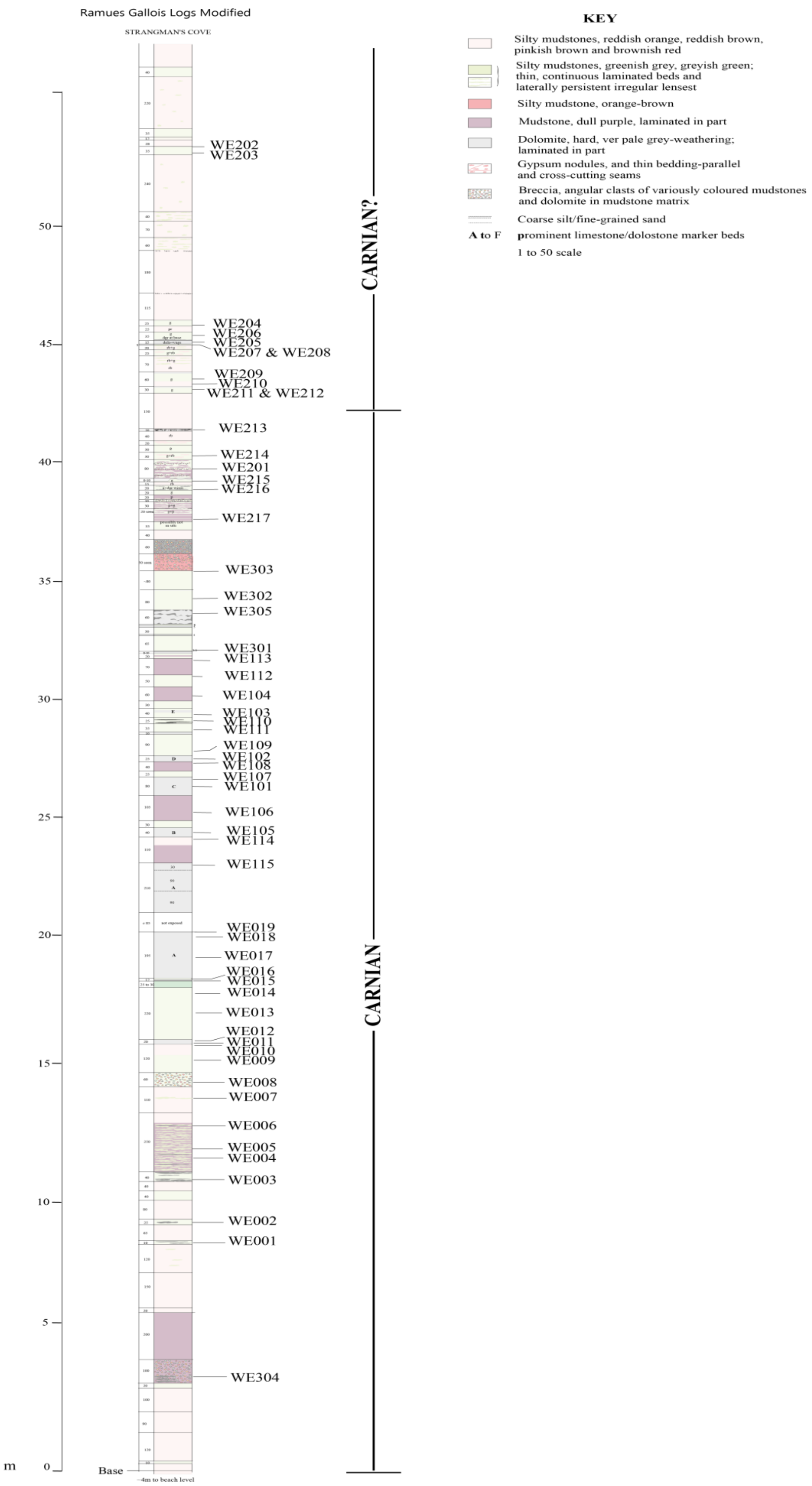

Figure 10: The lithological log of the studied outcrop and the position of the samples (modified from Gallois unpubl. of Weston outcrops in S. Devon)

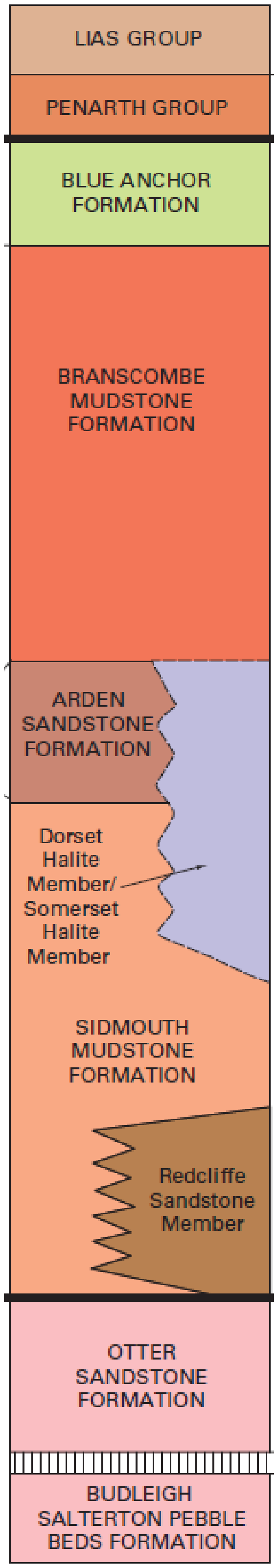

Figure 11: Lithological subdivision as proposed by Howard et al. (2008). The Arden Sandstone Formation is the equivalent name for Dunscombe Mudstone Formation, including the Lincombe Member.

The Arden Sandstone Formation comprises of grey, green and purple mudstone interbedded with paler grey-green to buff-coloured siltstone and fine to medium-grained, varicoloured sandstone (green, brown, buff, mauve). The lowest boundary is marked by the occurrence of breccias which have most likely been formed due to simultaneous halite solution. Previous works (Gallois and Porter, 2006; Howard et al., 2008; Porter and Gallois, 2008) have reported extensive bioturbation, soft sediment deformation structures, macrofossils and cross-bedding. The field observations of the present study were insufficient to confirm entirely the presence of sedimentological structures. On the one hand, the weathering of the outcrop by meteoric waters as well as the landslide effects are held responsible for having destroyed well-exposed parts, but on the other hand they contributed in uncovering new, previously unexposed, parts. Some parts of the outcrops were covered by vegetation, which again worked as a factor limiting the field observations. The Lincombe Member (Fig. 4) could be described as a sandstone body with lenticular geometry and a maximum thickness of approximately 5 m. The top boundary of the formation is bounded by another breccia as seen in fig. 10 between 49-50 m.

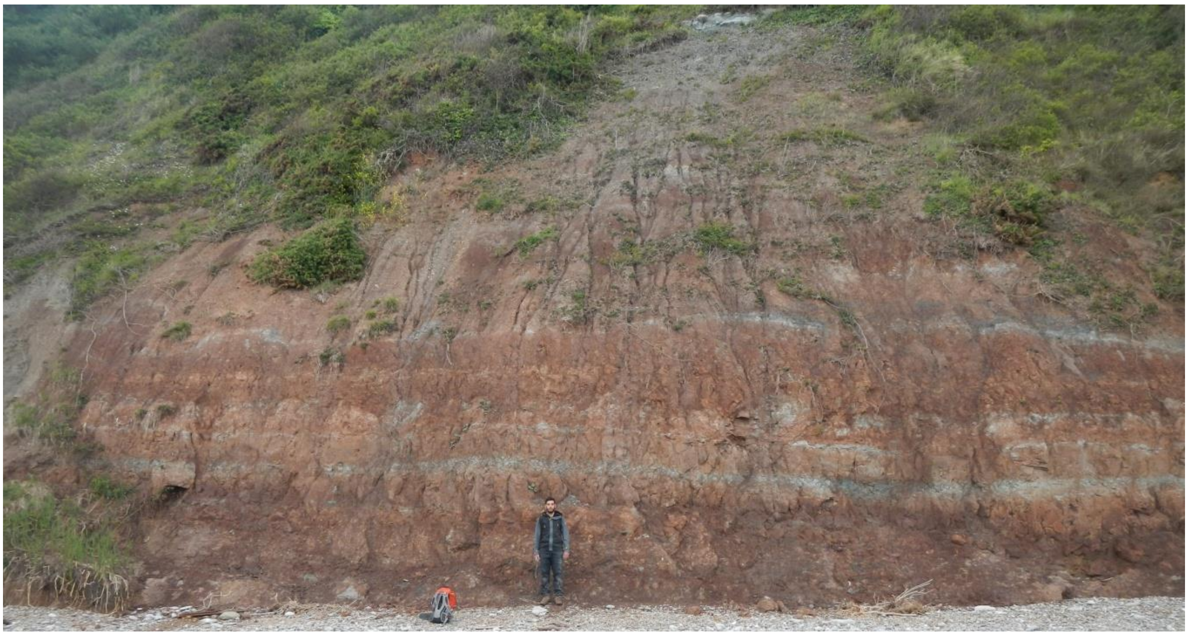

Figure 12: General example of the Mercia Mudstone Group; this is not the sampled outcrop

Figure 13: Green and red mudstones with calcitic concretions within Mercia Mudstone Group

Figure 14: Red and green mudstones with Mercia Mudstone Group

3. Material and methods

3.1. Samples collection

The samples were collected from two outcrops in the area of South Devon in Southwestern England (Fig. 3). The first outcrop is located on the Lower Dunscombe Cliff between Hook Ebb and Weston Mouth and the second on the Weston Cliff slightly east of Weston Ebb (Fig. 4 outcrops B and A). The fact that samples come from an outcrop instead of a core can prove to be favourable for clay mineral analysis since cementation can cause many alterations on the clay mineral assemblages.

In total 56 samples were taken from the outcrop out of which, 46 were destined for palynology, 22 for clay mineral analysis and 7 for thin section analysis. All the sample preparation techniques were carried out at the University of Oslo, Department of Geosciences. All remaining sample material, microscopic slides and thin sections are stored at the University of Oslo.

3.2. Palynofacies and palynology

Palynofacies analysis is based on transmitted light microscope study of organic particles concentrated by acid and basic solutions (e.g. Sebag et al., 2006 and references therein). The main goal is to quantify the various organic constituents (Sebag et al., 2006; Tyson, 2012) by counting and utilize the results for an attempt to reconstruct the depositional environment and trace potential palaeoclimate changes. The organic particles are characterized by diverse morphology, colour, opacity, size and distinct biological structures.

A total of 46 samples were analyzed for palynofacies. The preparation took place at the Palynology Laboratory of the Department of Geosciences, University of Oslo and the method employed included crushing, weighing (~8 gr), hydrochloric (30%) and hydrofluoric acid (37%) treatment and sieving with a 15 μm mesh sieve, all in accordance with standardized processing standards (e.g. Kuerschner et al., 2007; Traverse, 2007; Mueller et al., 2014). In addition, heavy liquid separation with $ZnCl_2$ had to be performed to separate the palynomorphs and organic material from the inorganic heavier mineral grains (pyrite etc.). 2 to 3 palynological slides for back-up reasons were produced for each sample depending on the quantity of the organic material. The optical microscopy analysis was done with a Leitz Wetzlar microscope and the equipment used for taking photos was an AxioCam ERc 5s camera connected to a computer using the software ZEN 2011. The software Tilia/Tilia Graph was used to produce the graphs with the relative abundances of palynofacies, palynomoprhs and algae (Mueller et al., 2015 and references therein). Using CONISS it became possible to differentiate between the different assemblages using cluster analysis within Tilia.

A quantitative method (counting) was applied for the study of particulate organic matter (OM). The minimum counting number of OM for each palynological slide was 300 and was subdivided in 8 categories. The organic material encountered was all of terrestrial origin and the categories are amorphous organic material (AOM), charcoal, wood, cuticle fragments, plant tissue, pollen, spores and algae. The origin of the AOM can vary depending on the sample from decayed pollen/spores, plant tissue, cuticle fragments, wood fragments and fresh-water algae. In my study, it seems most likely for AOM to originate from degraded algae. In addition, charcoal particles can also be affiliated with various groups, but regardless of the shape they are categorized as charcoal due to their dark black colour and opaque nature. Organic particles recognized as plant, wood or cuticle fragments had to bare visible plant-affiliated structures, brown colour (dark or light) as well as some transparency under the light microscope. Organic particles recognized as charcoal are black in colour, completely opaque under the light microscope and often, blade shaped. Some organic particles with those characteristics were defined as charcoal regardless if they bared plant-related structures. Defining an organic particle as AOM or algae (e.g. *Botryococcus)* is sometimes controversial. The main criterion used was the amount of gelification of the organic matter and the structure. In some cases, the structural features of *Botryococcus* are clearly visible, while in some others the only element pointing towards algae-related origin is just the high gelification of the organic matter. Nevertheless, both gelified AOM and algae have common origin, thus it should not blunder much with the results of the study.

3.3. Mineralogy

3.3.1. Bulk powder X-ray diffraction

For the clay mineral analysis 21 rock samples were prepared for powder X-ray diffraction (XRD). For the preparation of XRD bulks the samples had to be crushed in a crushing machine at University of Oslo for approximately 30 seconds. The next step was micronizing with a McCrone Micronizing Mill for about 10 minutes and then allowing the samples to dry out in an oven with maximum temperature 45°C to avoid any alteration of the clay minerals. The last step was the preparation of XRD. For separating the clay fraction (<2μm) the samples had to be crushed manually, dissolved in a Na_2CO_3 (0.125 g/L) solution, be left undisturbed for approximately 7h for the clay minerals to settle down and eventually collect the first 6.5 cm from the bottom of the beaker.

The XRD bulk and clay bulk analyses were carried out the XRD laboratory at the University of Oslo. The XRD bulks were run one time in order to get a graph for each sample. The clay bulks were run two times; air-dried, under ethylene-glycol (EG). The graphs originated from XRD bulks and clay bulks were studied in the Bruker EVA 2.0 software using the PDF2 database for phase identification. Profex software was used for more detailed modelling and quantification of the mineralogical phases based on the BGMN Rietveld code.

The identification of the mineral phases was primarily determined by the peak pattern of each mineral as reported in literature. The two main guidelines followed for the identification of the mineral phases were (Moore and Reynolds, 1989; Wilson, 2013). The peaks can be calculated either in 2-Theta or d values. The preferred way for calculations for this study is d values. Although each mineral is characterized by a pattern of peaks, there is always one main peak which is the most characteristic for each phase. All the mineral components identified in the study along with their main peaks are presented on Table 3 in Appendix. Some of the phases need more than one main peak to be distinguished. The reason for this is that sometimes a peak of a specific mineral can be masked by the peak of another mineral. For example, both kaolinite (kao) and chlorite (chl) in air-dried samples have a main peak at ~7 Å, so in case both are present it is necessary to notice a peak at ~14 Å which would confirm the presence of chlorite in addition to kaolinite. In this study, a supplementary way for distinguishing kaolinite from chlorite when both are present, is to check if there is a smaller peak slightly left from the main 7 Å peak. That is considered to be the kaolinite peak. The models derived from EVA and Profex programs were also used as guidelines for identification. More specifically, they were very helpful to distinguish ankerite/dolomite (ank/dol) in air-dried samples; determining which of the two precisely is not presented in the study. Quartz (qtz) is relatively easy to identify from its main peak (~3.34 Å) in air-dried samples. K-feldspars (K-feld) such as orthoclase and microcline (grouped together as k-feldspars), were recognized by their signature peaks at 3.21/3.24/3.29 – 3.31 Å at air-dried samples. Calcite (cal) is easily recognizable by its peak at ~3 Å in the air-dried samples which cannot be confused with any other. The calcite identified in the samples was mostly Mg-rich. Illite (ill) is recognizable by its sharp peak at ~10 Å in the air-dried condition. Sepiolite (sep) is recognized by its distinct peak at ~12 Å in the air-dried samples. Hematite (hem) is recognized by its peak at 2.70 Å in the air-dried condition. Sylvite (syl) is identified by the 3.14 Å peak and pyrite (pyr) by the 2.71 Å peak (both air-dried conditions). Smectite (sme) was identified on the EG samples when the 14 Å peak of chlorite in air-dried condition, diminishes and shifts towards the 16 Å under the EG effect. The broader this 16 Å peak the more smectite is present. However, smectite is identified qualitatively and not quantitatively in this study.

3.3.2 Thin sections

In total 7 dolomitic layered siltstone/sandstone samples were processed for thin section analysis. All thin sections were taken from samples of the dolomitic sections. Generally, the mudstones were quite unconsolidated whereas the dolomitic layers were laminated and consolidated enough to be processed for thin section analysis. The thin sections were produced at the thin section lab at the Department of Geosciences, University of Oslo and have been made perpendicular to the lamination of the samples. The equipment used was a Leitz Wetzlar microscope and an AxioCam ERc 5s camera for shooting the photos. The main magnification used for conducting the specific analyses was x10 and a bigger magnification of x40 was used for detailed studies. The reason for this is the low quality image of the micritic material under the high magnification. In addition, an optical microscope with crossed nicols availability was used for more detailed study of the thin sections.

A guideline from (from Milroy and Wright, 2002) was used for the analysis and description of the thin sections (figs. 9, 10). The authors conducted the research in Clevedon coast of the Bristol Channel (in Late Triassic rocks), which is not very far from the study area of the present work. It is suggested (in Milroy and Wright, 2000; Milroy and Wright, 2002 and references therein) that although lacustrine ooids are very rare in the fossil record, Mercia Mudstone Group (MMG) is a valid example for this. Some authors have interpreted MMG's ooids as a result of either deposition under marine settings or marine incursions (e.g. Warrington, 1970; Jeans, 1978; Leslie and Spiro, 1993). The present study follows the concept of the lacustrine origin for the ooids according to Milroy and Wright (2002).

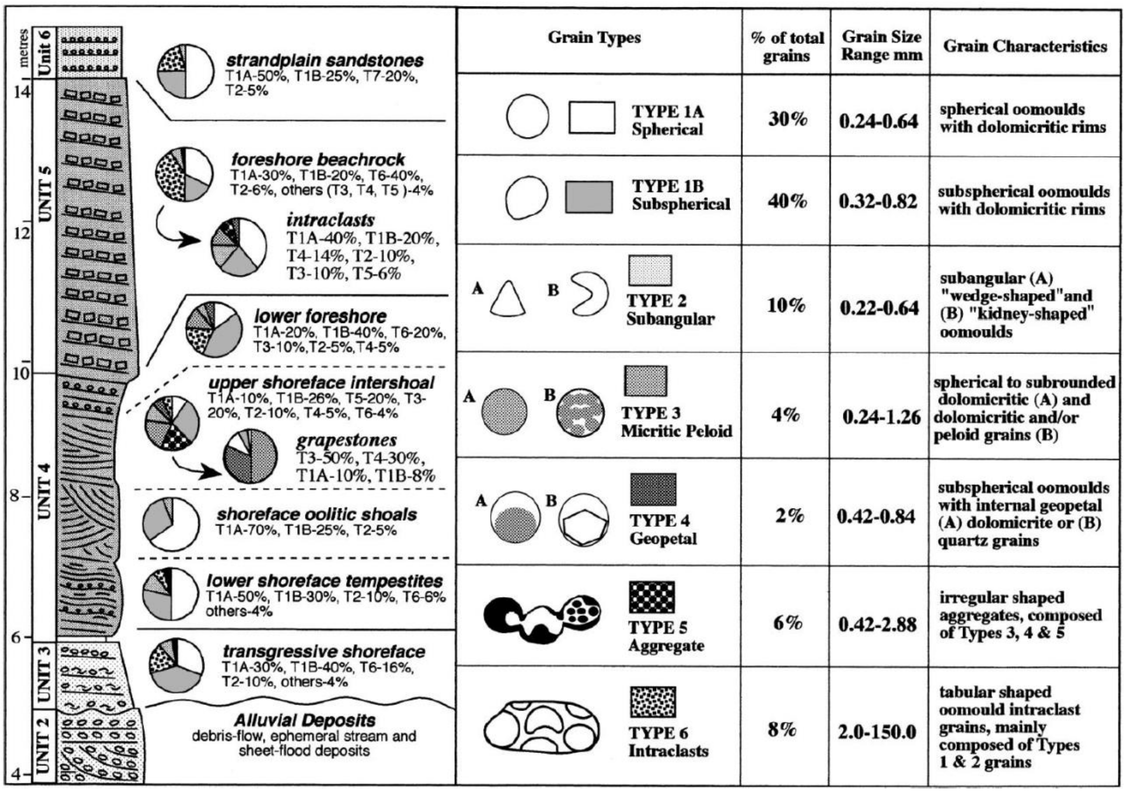

Figure 15: An example of a composite sedimentary log of the Clevedon Oolite showing changes in the distribution of grain types and assemblages from shoreline faces of a lacustrine lake (from Milroy and Wright, 2002).

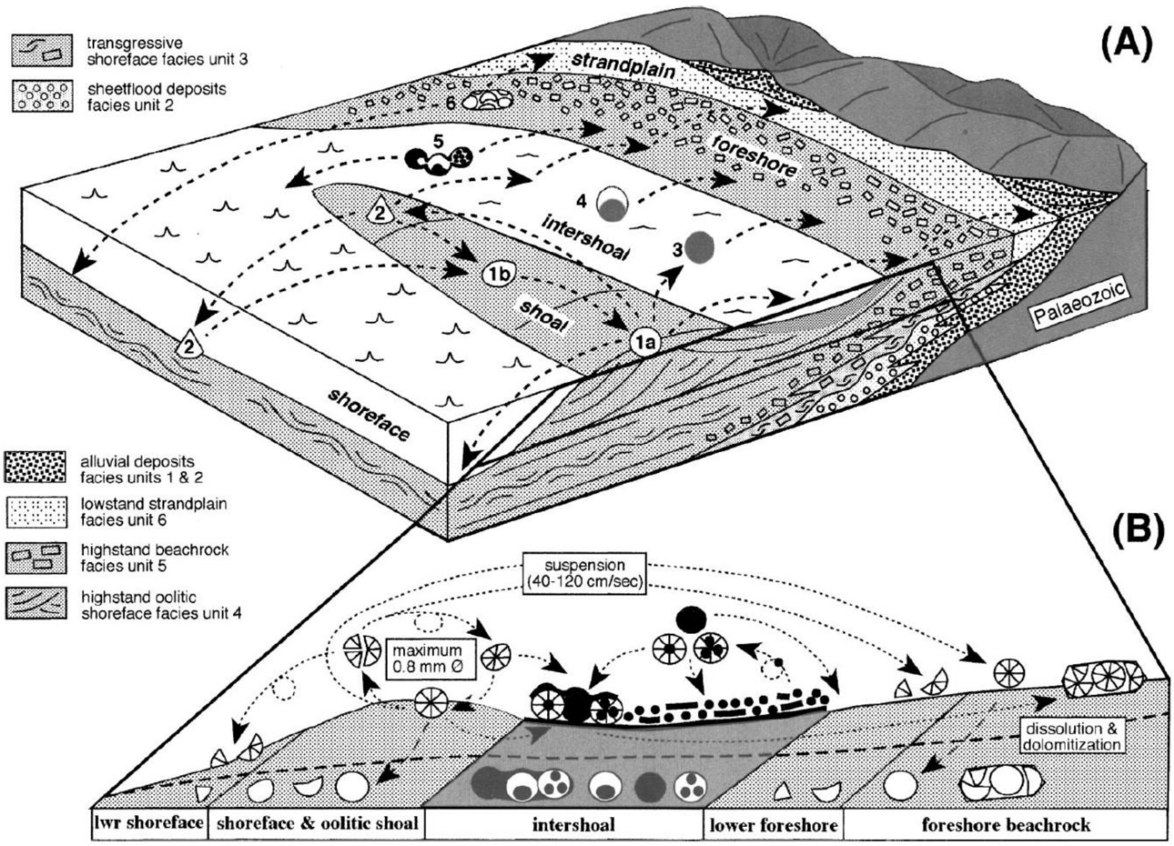

Figure 16: Example of the reconstruction model for the Clevedon palaeoshoreline (from Milroy and Wright, 2002).

4. Results

4.1. Palynofacies

4.1.1. Log and graph

The studied interval can be divided into two main groups as suggested by the counting data and the CONISS graph (fig. 17). Each group represents a large, general trend which is most profoundly defined by AOM, charcoal and pollen percentages. Even though the first sample is at 4 m, the division into groups starts from 9 m since no samples were collected in-between. **Group A** starts approximately from sample WE001, ends at approximately at sample WE114 and can be further subdivided in three smaller assemblages A_1 and A_2 and A_3.

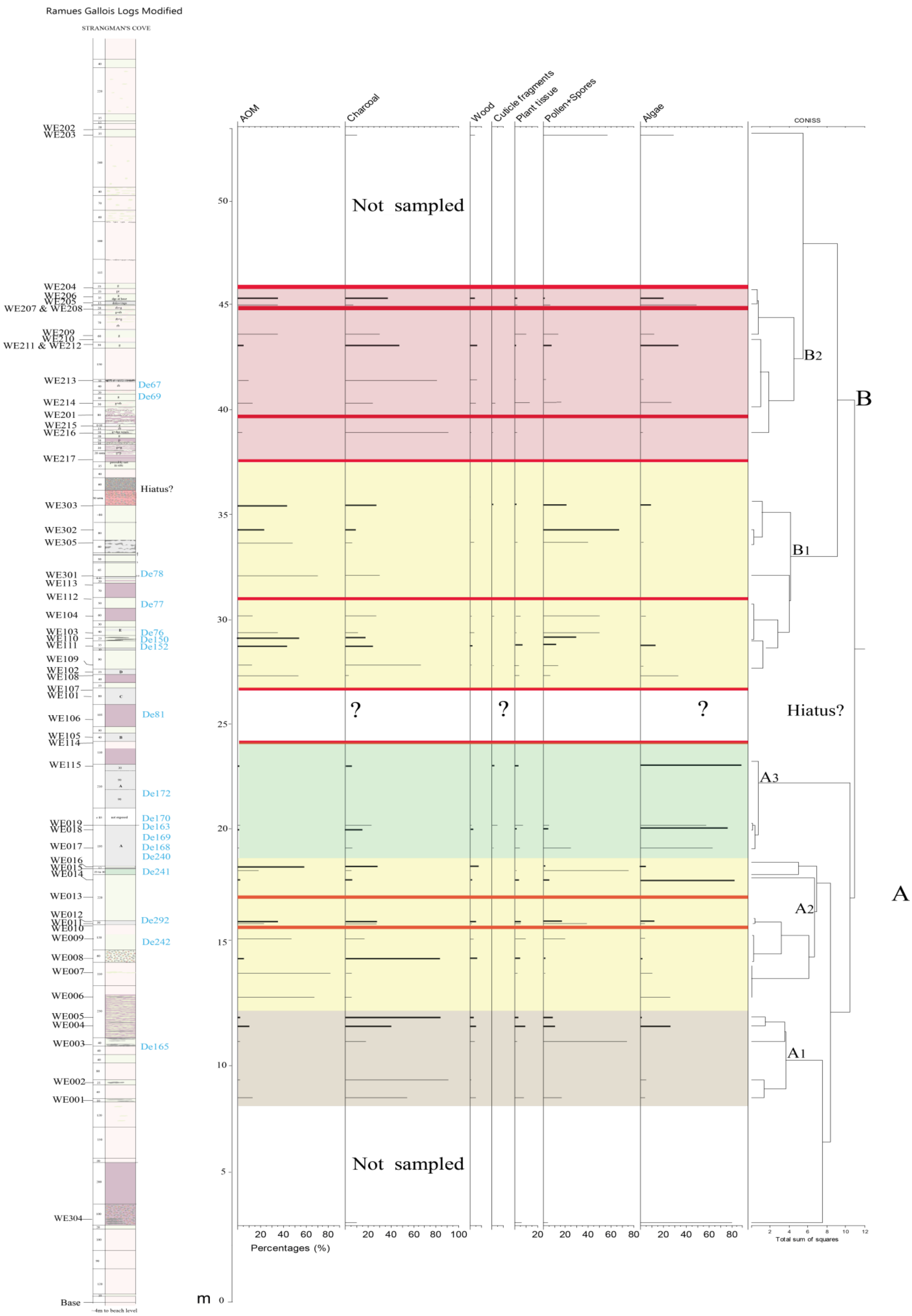

Figure 17: The lithological log next to the palynofacies graph. Samples De are explained in Table 2 in the Appendix.

A_1 assemblage includes samples WE001, WE002, WE003, WE004 and WE005. It is generally dominated by high charcoal values up to ~90% (WE002). There is only one sample WE003 that is dominated by pollen (WE003) up to ~80%.

A_2 assemblage starts from sample WE006 and terminates at sample WE016. It is characterized by high percentages of AOM up to ~85% (WE007) with one exception; sample WE008, which is rich in charcoal (~90%). The samples of the upper part of the assemblage (WE011–WE016) show a more mixed character and might mark the transition to the next group (A_3) that is distinctively richer in algae. Sample WE014 in particular is very rich in algae with ~80%. Samples WE010 and WE013 are barren. Nevertheless, the AOM percentages maintain high values on average throughout this assemblage. *Plaesiodictyon* is present in this assemblage (see ch. 4.3 for details).

A_3 assemblage includes WE017, WE018, WE019, WE115 and terminates at the barren sample WE114. It is mainly dominated by algae with up to ~90% (WE115), while the rest of the components are represented by significantly low values. Especially AOM is very scarce. *Plaesiodictyon* is present here.

The interval from WE114 to WE107 has not been sampled in the outcrop. Sample De81 from Fisher (1985) is placed between the samples WE114 and WE107 and is also barren.

Group B starts from approximately WE101 and terminates at WE204 (barren sample) and is subdivided in two smaller assemblages B_1 and B_2.

B_1 assemblage includes samples WE101, WE107, WE108, WE102, WE109, WE 111, WE110, WE103, WE104, WE112, WE113, WE301, WE305, WE302, WE303 and the barren sample WE217. It is characterized by high values of pollen grains and AOM. Pollen percentage values can reach up to ~65% (WE302). There is only one sample that is devoid of pollen and it has only AOM and charcoal (WE301).

B_2 assemblage includes samples WE216, WE215, WE201, WE214, WE213, WE212, WE211, WE210, WE209, WE208, WE207, WE205, WE206 and WE204. It is characterized by high charcoal values up to ~90% and simultaneously displays an increasing trend of AOM and algae from the lowest to the highest part.

Above sample WE204, there have been two more samples collected at approximately 53 m. The distance between WE203 and WE204 is so great that it is unreliable to include them in B_2.

4.1.2. Ternary plot

In addition, the above analyzed assemblages are plotted on a ternary plot (fig. 18). The three main components were ‘AOM & algae’, ‘palynodebris’ and ‘terrestrial palynomorphs’. AOM and algae were categorized together because of their close affiliation (why, referecne). AOM tends to originate from degraded algae (*Botryococcus*). The ‘palynodebris’ component is the total grouping of charcoal, wood, plant and cuticle fragments counted in each sample. The ‘palynomorphs’ component consists of pollen and spore grains together.

Samples from assemblage A_1 are widely distributed along the line between ‘AOM and algae’ and ‘palynodebris’, with one exception plotted close to ’palynomorphs’ and ‘palynodebris’ line (WE003).

Samples from assemblage A_2 are mostly concentrated along the ‘AOM and algae’ and ‘palynodebris’ line, but more closely to ‘AOM and algae’ corner. There are a few samples plotted near ‘palynodebris’ corner (WE008) or near ‘palynomorphs corner (WE015) breaking the pattern.

Samples from assemblage A_3 are strictly plotted near the ‘AOM and algae’ corner and that is because this is an algae-rich interval. *Plaesiodictyon* is present here (see algae results chapter for more).

Samples from assemblage B_1 are widespread around the center of the ternary plot showing a multicomponent character. Some can be near corners, such as sample WE108 (‘AOM and algae’ corner) or WE301 which is devoid of pollen and spores. WE301 is special, because the AOM found in this sample is of unknown affinity. It does not seem to relate to *Botryococcus*, and it is hard to define if it does since there are no algae particles for comparison.

Samples from assemblage B_2 are largely distributed along the line between ‘AOM and algae’ and ‘palynodebris’. The reasons are the steadily low values of pollen and spore grains.

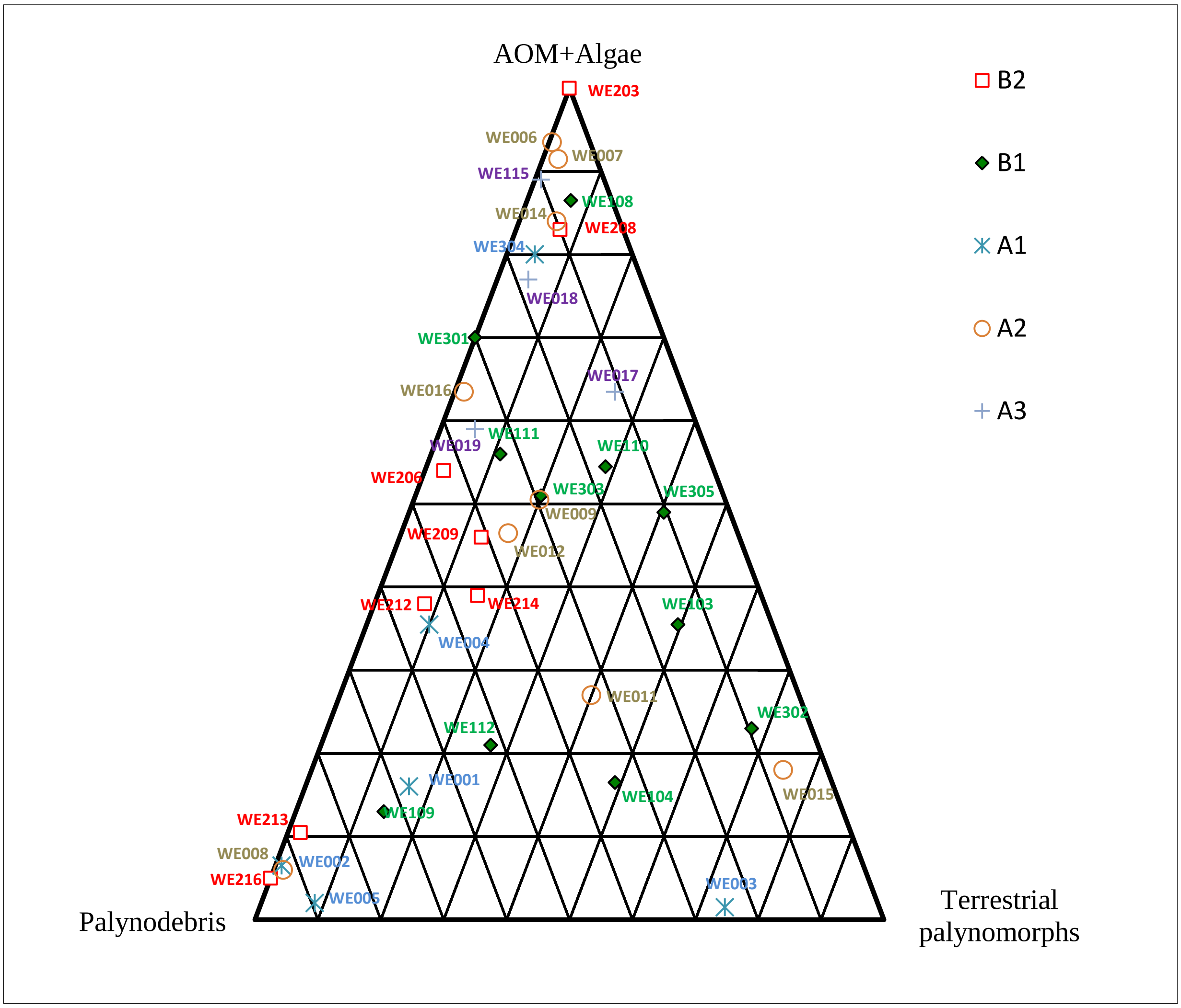

Figure 18: Ternary plot featuring three components: i) AOM and algae, ii) Palynodebris, iii) Palynomorphs. The various tick marks represent the different assemblages as determined in Chapter 'Palynofacies results'

4.2. Palynology

A preliminary qualitative palynological analysis was carried out in order to provide a basis for comparison between the present study and Fisher (1985) and the results are presented in fig. 19. The various forms of bisaccate pollen are not being distinguished separately. The forms identified in this study are bisaccates, *Calamospora* sp., *Dupliciporites* sp., *Enzonalasporites* sp., *Ovalipollis* spp., *Porcellispora* sp., *Praecirculina* sp. and *Triadispora* sp. (see detailed description and systematic taxonomy in chapter 5.1). The samples being analysed for palynology are presented on Table 2 with stratigraphical order from bottom to top along with the corresponding samples from Fisher (1985).

The palynological results of this study are closely related to the results of Fisher's (1985) study (fig. 19). First of all, the three barren samples identified in the present study correspond to those of Fisher (1985), with the minor difference that in De292 and De81 he has noted only the presence of *Ovalipollis* and bisaccates respectively, but without having included them in his quantitative analysis (see Fisher, 1985 for details). The sample WE301 contains only charcoal and AOM and therefore ties well with the De78 which is defined as barren by Fisher 1985. The rest of the samples are closely related as well and this can be seen where circles and crosses are matching under the same genus. Some of the differences lie mainly in some extra bisaccate forms identified by Fisher (1985). Those are included in the ‘bisaccates’ category and are not identified separately in this study.

According to the results after the qualitative palynological analysis, it is feasible to divide the section in three different assemblages. The division begins from WE003 and above. Below that point there are no data. For correspondence between the palynological slides of the present study and Fisher’s 1985 refer to Table 2 in the Appendix.

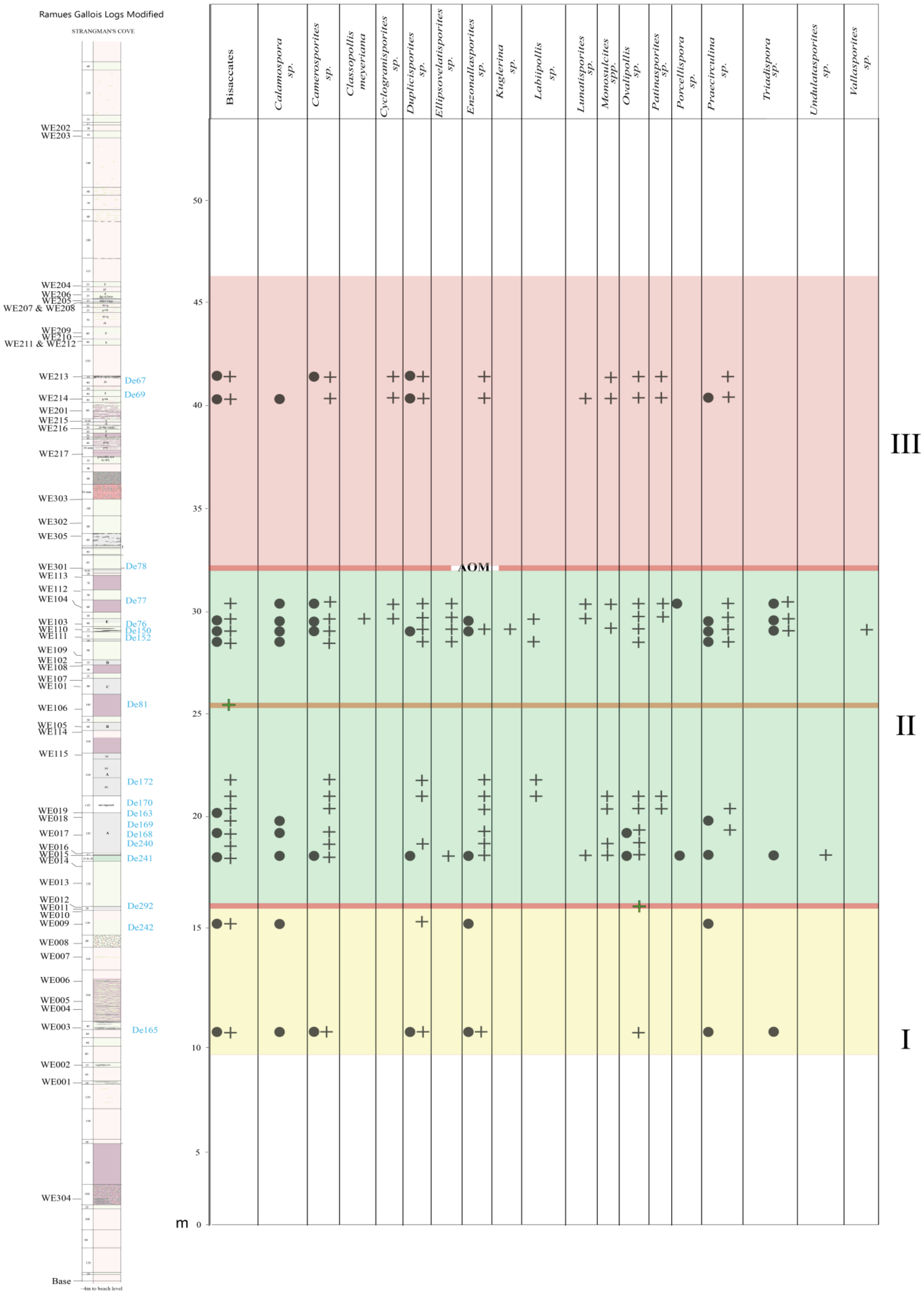

Figure 19: The lithological log next to the palynology graph. Samples from the present study are symbolised as circles, samples from Fisher (1985) as crosses.

Assemblage I starts from sample WE003 and terminates at WE011 (barren sample). The results are based on only two samples (WE003 and WE009) due to the scarcity of pollen and spore grains in the rest of the samples. The palynomorphs encountered in this assemblage are bisaccate pollen, *Calamospora* sp., *Camerosporites* sp., *Duplicisporites* sp., *Enzonallasporites* sp., *Praecirculina* sp. and *Triadispora* sp.. In this interval, Fisher (1985) has additionally identified the *Ovalipollis* genus, which does not correlate with my analysis.

Assemblage II starts right above the barren sample WE011 (De292) and terminates at WE301 (De78). Sample WE011 is barren, while in sample De242 Fisher mentions just the presence of *Ovalipollis* without mentioning any additional quantitative result. Assemblage II includes samples WE015, WE017, WE019, WE111, WE110, WE103 and WE104. The palynomorphs identified are bisaccate pollen, *Calamospora* sp., *Camerosporites* sp., *Duplicisporites* sp., *Enzonallasporites* sp., *Ovalipollis* sp., *Porcellispora* sp., *Praecirculina* sp. and *Triadispora* sp.. Fisher in his study (1985) has additionally identified some other forms (*Ellipsovelatisporites* sp., *Labiipollis* sp., *Lunatisporites* sp.), *Classopollis meyeriana* (mentioned as *Corollina meyeriana* in his study), *Kuglerina* sp., *Cyclogranitisporites* sp., *Monosulcites* sp., *Patinasporites* sp., *Undulatisporites* sp. and *Vallasporites sp.*. The two extra genera identified by me in this interval, and not by Fisher (1985), are *Calamospora* sp. and *Porcellispora* sp.. The barren sample WE106 corresponds with De81 in which Fisher (1985) mentions just the presence of bisaccates. The end of the assemblage is marked by sample WE301 which consists only of AOM and charcoal. The AOM in this sample could either be marine or terrestrial.

Assemblage III starts above WE301 and terminates at approximately where sample WE204 is. This assemblage includes WE214 and WE213 samples, but in general the pollen and spore values are very low (fig. 17). The genera variety is low accordingly. The palynomorphs identified are bisaccate pollen (undifferentiated) and *Calamospora* sp., *Camerosporites* sp., *Duplicisporites* sp. and *Praecirculina* sp.. Fisher (1985) identified in addition Lunatisporites sp., *Ovalipollis* sp. (bisaccate forms), *Cyclogranitisporites* sp., *Enzonalasporites* sp., *Monosulcites* sp. and *Patinasporites* sp.. The only extra genus identified in the present study, and not in Fisher's (1985), is *Calamospora* sp.. From the sample WE204 and up, no palynological analysis was conducted.

4.3. Fresh-water algae

Based on the identification of *Plaesiodictyon* sp. and *Botryococcus* sp., a division of the section into three categories A, B and C was made (fig. 20).

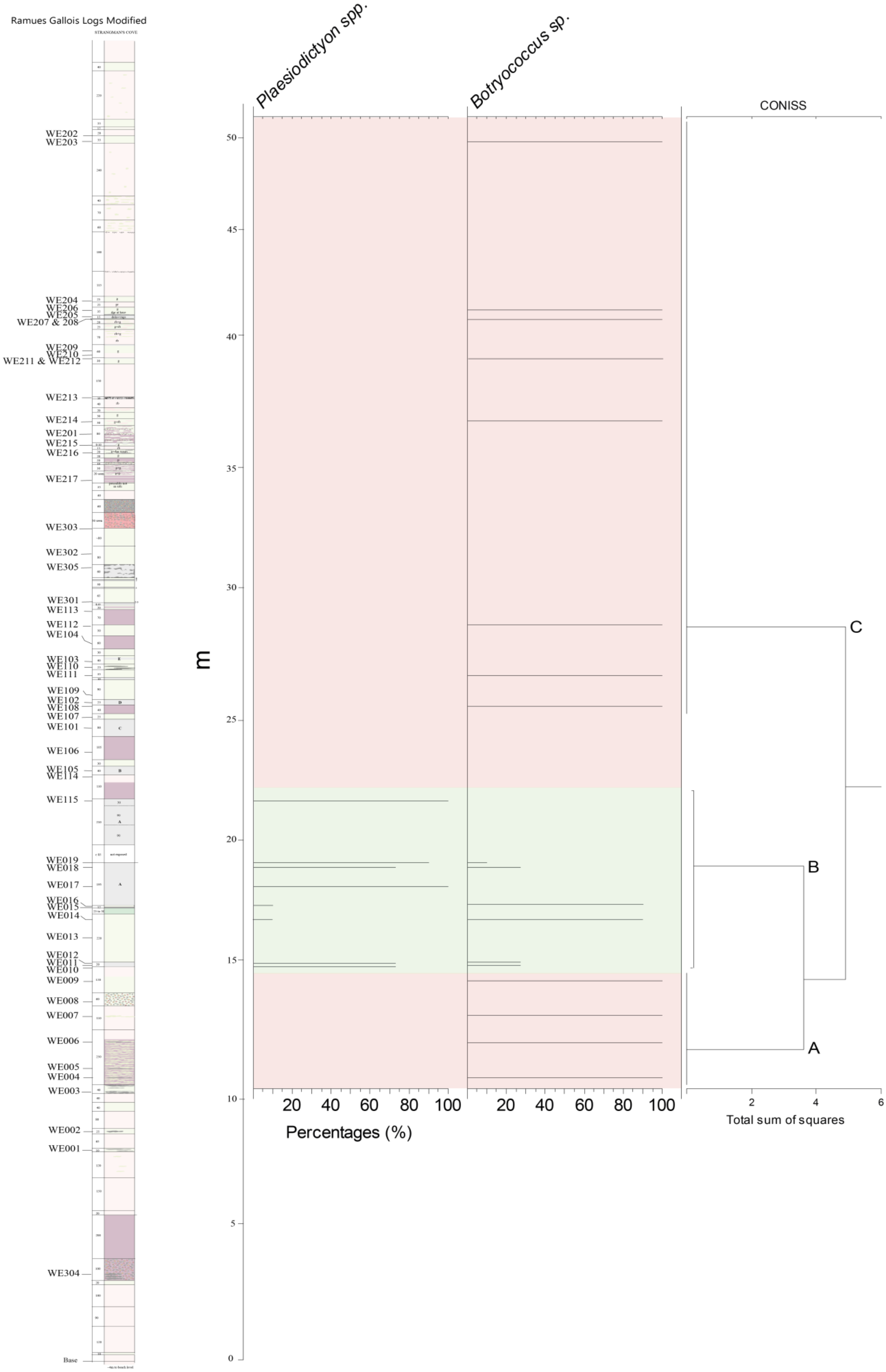

Figure 20: The lithological log next to the algae graph

Assemblage A starts from sample WE003 and ends at sample WE009. It includes samples WE003–WE009. The assemblage is dominated by *Botryococcus* sp. that in many cases is represented by clear examples but very often it becomes difficult to distinguish it from AOM. In order to make such decisions, the texture of the particles was additionally considered. The more gelified a particle is, the more likely is to be *Botryococcus* sp..

Assemblage B starts from sample WE010 and ends at sample WE115. It is marked by the appearance and disappearance of *Plaeisiodictyon* sp. and it is actually the only part that this alga is present throughout the whole section. Samples WE017 and WE115 are dominated by *Plaeisiodictyon* sp.. Samples WE010, WE012, WE016, WE018 and WE019 show mixed *Plaeisiodictyon* sp. with *Botryococcus* sp., *Plaeisiodictyon* sp. is dominant even in those mixed samples with percentages around 70–80 %. In two of those samples (WE014, WE016), however, *Botryococcus* sp. takes over with ~90 %.

Assemblage C starts from WE108 and ends at WE203. It includes samples WE108, WE111, WE112, WE214, WE212, WE208, WE206 and WE203. It is similar to assemblage A and is dominated by *Botryococcus* sp.. Some samples are represented by significantly gelified specimens such as WE108, WE111, WE112, WE206 and WE203.

4.4. Mineralogy

4.4.1. XRD clay bulk samples

The XRD bulk data are presented on a bar graph (fig. 21) next to the lithological log. The graph shows the percentages of the minerals based on their peaks as identified on EVA and Profex programmes. From the variations in the values of the mineral component the complete section can be divided in three mineral assemblages; i, ii and iii.

Figure 21: The lithological log next to the mineralogy graph. Marked with green are the smectite-rich samples and with orange the samples with low, but still considerable amount of smectite. The rest have trace amounts of smectite.

The mineral assemblage i starts from sample WE001 and terminates at sample WE015. The mineral components present here are qtz, cal, ank/dol, kao, chl, ill, k-feld and sep (abbreviations explained in ch. 3.4). The main features of this assemblage are the relatively higher values of sep from ~0.1 up to ~10% (compared to the other assemblages) and the distinct presence of ank/dol from ~5 up to ~63%. The samples WE011, WE013 and WE015, however, show low values of sep such as 0.103, 1.25 and 1.14 respectively. Sample WE007 does not contain any sep. Furthermore, sample WE001 is the only one having a low percentage of ank/dol with 4.83%. Qtz values vary significantly from <1% (WE011) up to ~42% (WE001). Cal is generally low between ~1 and 5% with sample WE009 as the only exception being richer up to ~21%. Chl values are stable between ~3–6%. Exceptions are sample WE007 with ~12% and sample WE011 with <1%. Ill is constantly present here as well and has values from ~8 up to 60%. Kao is present in three samples (WE304, WE003 and WE015) with ~0.5, 0.2 and 1.5 values respectively. K-feld retains percentages from ~8 to 30% with sample WE011 as an exception (<1%). Hem, pyr and syl are not present in this assemblage.

The mineral assemblage ii starts from sample WE115 and terminates at sample WE303. The mineral components present here are qtz, cal, ank/dol, kao, chl, ill, K-feld, sep, hem, pyr and syl. The mineral phases in this assemblage vary greatly. K-feld and chl are the only phases retaining a relatively stable character. K-feld ranges from ~12 up to 32% and chl from ~3 up to 11%. Qtz varies from ~8 up to 32%. Ill maintains a stable presence as well with values between ~13 and 23%. Ank/dol shows significant variations from ~5 up to 56% while Cal ranges from ~1 up to 27%. Cal is absent in samples WE109, WE113 and WE301. Sep is present with percentages from <1 up to 3% approximately and it is completely absent in samples WE115, WE113 and WE305. Kao is present in samples WE113, WE305 and WE303 with ~2, 0.5 and ~3% respectively. It is absent in the rest of the samples in this assemblage. Hem is identified only in sample WE303 (~2%), pyr in samples WE110 (~0.5%), WE305 (~0.3%) and syl in samples WE110 (~0.2%) and WE301 (~0.3%).

The mineral assemblage iii starts at WE214 and terminates at sample WE203. The mineral components present here are qtz, ank/dol, cal, kao, chl, ill, K-feld, sep and hem. The mineralogical phases of qtz, ank/dol, chl, ill and K-feld are present throughout the whole assemblage. Qtz maintains steady between ~8–14%. Cal is present only in samples WE214 (~7%) and WE203 (~31%). Ank/dol ranges from ~5 up to 36%. Kao exists only in sample WE203 (~4%). Chl ranges from ~5 to 6% and K-feld from ~20 to 29%. Ill values range from ~17 up to 22%. Sep exists only in samples WE206 (~1%) and WE203 (<1%). Hem is present only in sample WE203 (<1%). Syl is present only in sample WE214 (<1%) as well.

A step further into the analysis of the clay minerals composition under the effect of ethylene glycole (EG) can indicate the presence of smectite. The smectite is being included under the chlorite percentages calculated in the air-dried stage and is only qualitatively identified by the ~16 Å broad peaks on the EG stage. The higher the 16-17 Å peak is, the higher the participation of smectite in the sample. The geometry of the peak, including height and broadness, can provide with information also about the type of smectite mineral or any mixed layers, but this is far too detailed for this study to cover. As inferred by the graphs (figs. 21 and 22), the smectite bearing samples are the following in descending order regarding the smectite proportion: WE304, WE007, WE109, WE110, WE301, WE013, WE011, WE009, WE106, WE303, WE015 and WE206. The samples that seem to have very small amounts (traces) or total absence of smectite, are: WE005, WE305, WE210, WE113, WE214, WE001, WE003, WE115 and WE203.

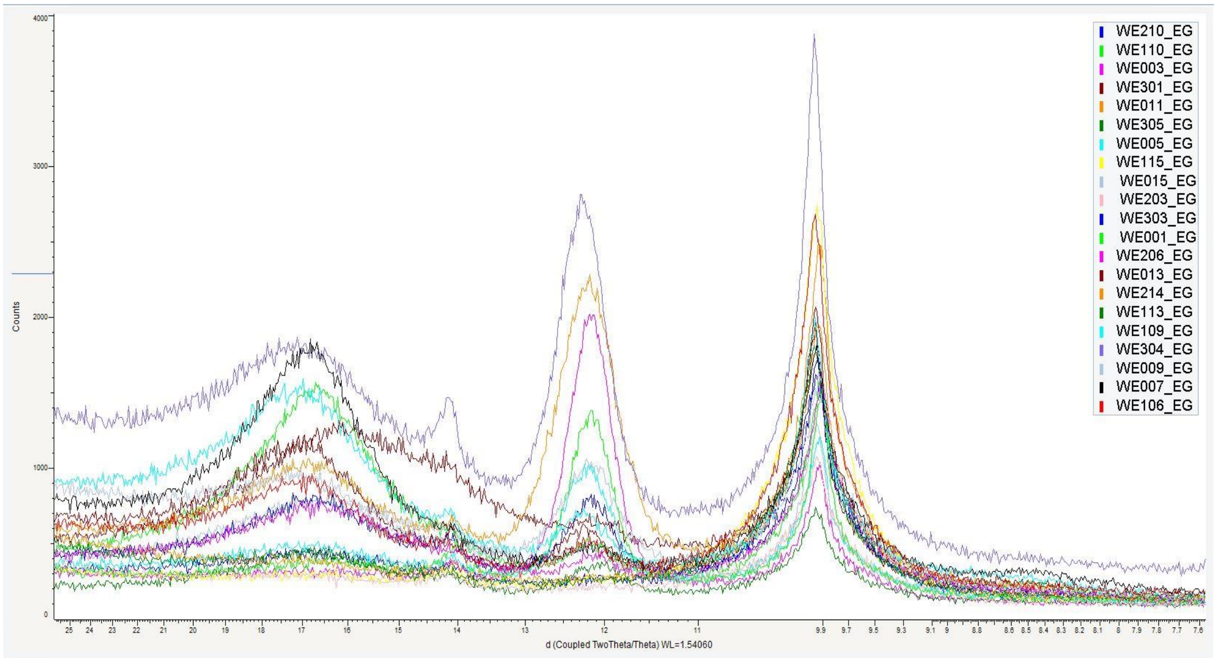

Figure 22: The samples under EG effect. The broad peaks around 16 Å indicate the presence of smectite.

4.4.2 Thin sections

The results are based on the descriptions from Milroy and Wright (2002, see fig. 15 for terminology of grain Types 1, 2, 3, 4, 5, 6). The analysis under light microscope gives extra information about the depositional environments. The description is presented from the stratigraphically lowest sample WE011 to the highest sample WE202. The samples analyzed on thin sections were WE011, WE012 and WE012b (all three are from the same horizon, b is the lower one between the two of WE012), WE101, WE215, WE206 and WE202. There is a plate (Pl. 5) in the Appendix showing pictures of each thin section.

- WE011: This sample is the lowest stratigraphically and it is taken from a dolomitic horizon. It contains ooids, Type 1 (~15%), aggragate grains (sparitic material), Type 5 (~15%) and micritic peloid material, Type 3 (~70%) (Pl. 5, figs. 1, 2).

- WE012b: This sample differs from the previous one. It contains aggragate grains, Type 5 (~40%), micritic peloid, Type 3 (~60%) (Pl. 5, figs. 5, 6). No ooids are found in this sample.
- WE012: This sample contains mainly micritic peloid grains, Type 3 (100%) (Pl. 5, fig. 4). No ooids are found here either.
- WE101: This sample contains mainly intraclasts, Type 6 (~75%) and aggragate grains, Type 5 (~25%). Ooids of bigger size are found here (~100 μm, Pl.5, fig. 7).
- WE215: This sample is dominated by micritic peloid grains, Type 3 (Pl. 5, fig. 10).
- WE206: Similarly to WE215, this sample is characterized totally by micritic peloid material, Type 3 (Pl. 5, fig. 9).
- WE202: This sample contains intraclasts, Type 6 (~65%) and aggragate grains, Type 5 (~40%). Calcite is identified here (Pl.5, fig. 8). Very few ooids are encountered, around ~10% of the thin section.

5. Discussion

Palynofacies and palynology

It can be inferred that palynofacies and palynology show variations in relation to the lithology and sedimentology. For instance, the dominance of fresh-water algae in assemblage A_3 is clearly coupled with a high variety of pollen and spores assemblage. Pollen and spores are characterized by high variety also in the bottom part of B_1 (fig. 17, 19) even though the lithology shifts from dolomite dominated to mudstone dominated respectively. This shows the climatic conditions were favourable all along the duration of this interval regardless the lithology alterations. The presence of *Camerosporites seccatus* throughout the section implies an age of Carnian (Kurschner and Herngreen, 2010). Charcoal abundances seem to show a connective pattern to lithology as they are highest on mudstone dominated lithologies (A_1, B_2) and most likely it also represents hotter climatic condition (intertinites are indexes of fires). It can therefore be concluded that those variations in palynofacies and palynological components are actual expressions of climatic fluctuations.

Clay minerals

The mineralogical component is also connected to the lithology and depositional environments. It is noteworthy that different lithologies either dolomite or mudstone dominated are accompanied by specific mineralogical phases respectively. For instance, the dolomite-dominated (Lincombe Member) samples are usually coarser grained (Gallois and Porter, 2006) and clay minerals like kaolinite, hematite, pyrite or sylvite are absent (e.g. sample WE115). On the contrary, mudstone-dominated samples tend to contain calcite, kaolinite, hematite, pyrite or sylvite. It is important to emphasize that the clay mineral compositions <2 μm are climatically controlled (Haas et al., 2012 and references therein). Haas et al. (2012 and references therein) refer to kaolinite and smectite as indicators of increased chemical weathering, while the predominance of illite and chlorite is interpreted as a marker for physical erosion. Moreover, Rostasi et al. (2011) refer to kaolinite as an index for a hot and humid climate and to smectite as a mineral phase formed in seasonal climates of wet and dry periods characterized by masses with low and poorly drained relief.

Optical microscopy

The interpretation of the thin section analysis results seem to be relevant to those defined by previous works (e.g. Gallois and Porter, 2006; Porter and Gallois, 2008) in regards of lithology and depositional environments. The most striking evidence which varied depending of the sedimentary facies was the presence or absence of ooids. Ooids were usually present in samples collected from dolomite-rich intervals and absent in samples from mudstone-dominated intervals, even though those samples themselves could represent a small, laminated, dolomite-rich part. Those types of lithology most likely correspond to ephemeral stream deposits in contrast to the more extended dolomitic intervals which may very well reflect fresh-water lake deposits (ooids presence as indication) under a more humid climatic setting.

Interpretation

The results of palynofacies and palynology analyses can be compared with the sedimentology and lithology. The interpretation is organized according to the palynofacies subdivision as this is the main focus of the study (fig. 17). The order is from stratigraphically lower to higher.

Assemblage A_1 is assembled predominantly by mudstones of variable colours (red, green, dark grey/black) and one breccia on the bottom part of the section (where sample WE304 is located, fig. 17). The lithology in this assemblage varies with many alterations existing between the different mudstone types (red, green, grey/dark grey). This, in combination with the palynofacies, palynological, mineralogical and thin section analyses implies changes in depositional environment which in turn is an outcome of climatic instability. The depositional environments here are determined as fluvial/lacustrine with ephemeral, shallow ponds and streams. Probably the dark laminated mudstones (for example samples WE001, W002, WE003, fig. 10) represent these small ephemeral ponds where *Botryococcus* is present. *Botryococcus* is known to be present in fresh (to brackish), clear waters with low circulation (Ji et al., 2010). This interpretation is in accordance with Gallois and Porter (2006) and Porter and Gallois (2008) conclusions based on ichnofacies and sedimentological criteria. The lack of evidence pointing towards well oxygenated waters in high energy environments, both in terms of palynology and sedimentology, indicates the palaeotopography was of low relief. Therefore, the small thickness of the mudstone layers could indicate the dominance of lateral variation over the vertical, which in turn shows steady rates of tectonics. Gallois and Porter (2006) mentioned already that the palaeorelief must have been low.

The presence of charcoal, along with the presence of pollen and spores, imply a climate wet enough to sustain vegetation (fig. 19) showing the small variety of pollen and spores). At the same time the dominance of charcoal, which can be considered as a fire indicator (inertinites) in most of the samples (fig. 17) can imply the occurrence of dry periods within this interval. The samples also plot near the 'palynodebris' corner in the ternary plot as a result of charcoal's high relevant abundance (fig. 18). The presence of kaolinite (kao), which is an index of weathering, proves the occurrence of periods with high precipitation (samples WE304 and WE003, fig. 21). Nonetheless, these wetter periods must have been either seasonal or short in connection to other parameters (e.g. astronomical, tectonics, global climatic changes). The total lack of smectite could indicate that, even though there were some periods with higher humidity, the climate must have been hot in terms of temperature. This is the only explanation considering the presence of kaolinite (hot and humid index according to Rostasi et. al 2011 and Haas et. al 2012).

Assemblage A_2 is mudstone-dominated and comprises of red, green and grey (laminated) mudstones (fig. 17). The alterations in lithology are less frequent than in A_1, thus indicating the prevailing vertical variations over lateral. The palynofacies relevant abundances imply high variety of organic particles, showing that the conditions were suitable for pollen and spores (vegetation), fresh-water algae (both *Botryococcus* and *Plaesiodictyon*) to be present. The alterations in the palynofacies relevant abundances can be explained by different depositional environments due to some minor lateral changes. More specifically, the bottom part of A_2 consisting primarily of red mudstones is dominated by AOM, charcoal and algae (from sample WE006 up to WE008, fig. 17), while the upper part consisting more of green mudstones is more pollen/spore-rich (from sample WE009 up to WE015, fig. 17). Between the two intervals there is one breccia (where the charcoal-dominated sample WE008 is in fig. 17) marking a change. It is shortly above this breccia, that *Plaesiodictyon* appears, possibly indicating a gradual transition to a more marginal lacustrine depositional environment (in agreement with Gallois and Porter, 2008). *Plaesiodictyon*'s abundance becomes progressively higher than the abundance of *Botryococcus* as seen in fig. 20. The gradual nature of this change makes the climate as the best candidate to be the cause. Ooids are found in sample WE011 corresponding to a thin, dolomite-rich layer (fig. 17), implying the presence of lake deposits. Right above, the absence of ooids in samples WE012b and WE012 account for an unstable setting. In sample WE015 (fig. 17) kaolinite (kao) is present and serves as evidence for humid conditions where chemical weathering occurs. In addition, smectite is very common in A_2.

Overall, in the bottom part of A_2 the climate shows a similar character to that of A_1, but slightly wetter as inferred by the prevailing of AOM over the charcoal relevant abundances. The shift towards a more humid setting is evident on the upper part of A_1, where the relevant abundances of pollen and spores increases and coincides with the dominance of *Plaesiodictyon* over *Botryococcus* as well as with the change of lithology from red-dominated to green-dominated mudstones. Similarly, the depositional environment changed from a fluvial/lacustrine to a marginal lacustrine as proved by the occurrence of ooids in the dolomite-rich layer, which might reflect the margins of a fresh-water lake.

Assemblage A_3 comprises solely of dolomitic layers, in coarser grained (field observation) and coincides with the also coarser grained Lincombe Member (Porter and Gallois, 2008). Despite the fact that palynofacies trends are dominated by algae, the palynological component of pollen and spores is characterized by high variety, implying that the conditions were favourable for the thriving of both vegetation and the fresh-water algae (mainly *Plaesiodictyon*). This is obvious also from the ternary plot for the A_3 samples which are concentrated mainly close to the 'AOM+algae' (fig. 18). The findings from this interval provide an interpretation coming to terms with Gallois and Porter (2008) that the depositional environment being lacustrine-deltaic reflecting the slightly deeper part of a big fresh-water lake.

It appears the climate in this interval is humid enough to allow the development of a lake system of considerable size. It is likely that the precipitation rates have increased significantly and reached a maximum compared with the past two assemblages (A_1 and A_2). Evidence for this is also the low values of the charcoal relevant abundances.

On top assemblage A_3 is a short interval (from samples WE014 up to WE107) bounded by barren samples, which has not been properly sampled in-between. The comparison with Fisher (1985) shows that sample De81 located in the middle of the interval is barren.

Assemblage B_1 is mudstone-dominated and consists of red, green and grey, dark laminated mudstones in alternations. The palynofacies and palynological indicators here are characterized by high a variation with equal ratios of AOM, charcoal and pollen/spores. The abundances of algae are low and *Plaesiodictyon* is absent. The pollen/spores maintain their high variety after A_3 reflecting a climatic setting favourable for vegetation to thrive. The samples on the ternary plot (fig. 18) are widely distributed around the center of the plot indicating variety in the palynofacies trends. The presence of kaolinite (kao) reaches its maximum in this interval (samples WE113, WE305, WE303, fig. 21) indicating increased precipitation. Smectite is still present in B_1 indicating that the eclimatic setting is being maintained through this interval as well. Big-sized ooids were present in sample WE101, which is located at the lowermost part of B_1 from a thin dolomitic layer. The depositional environment seems to be shifting back to a more marginal lacustrine (again in agreement with Ramues and Gallois, 2008).

The evidence point towards a climate of high humidity and precipitation, which raises the question why did the lake deposits not continue being present in the extend it was in A_3 provided the climate is humid in the same or even higher degree. This can be interpreted in three ways: i) This lake system moved laterally and cannot be traced in that part of the outcrop, ii) The tectonics became more active and caused uplifting of the area in a rate so high that the lake could not keep up, iii) There was a regression event forcing the lake sedimentary facies to retrograde towards the sea.

Taking into account the results of the study, it appears that the humidity level of the climate at the time was still high (perhaps even higher) following A_3 as reflected by the high variety of pollen/spores, AOM (which most represents degraded algae as mentioned in Ch. 2), the high participation of kaolinite (kao) and the presence of big-sized ooids. Furthermore, the sylvite (samples WE110, WE301) and the pyrite (samples WE110, WE305) that were detected in B_1 imply quick, abrupt climatic shifts from periods of high precipitation to drier periods when evaporation prevailed. The hematite found in sample WE303 that happens to come from a brecciated horizon apparently represents an interval exposed to air. The studied section is of Carnian age (Hounslow et al., 2002; Gallois and Porter, 2006) based on palaeomagnetic data. Those brecciated horizons can represent a hiatus which can explain the considerable presence of hematite (notice that hematite is at its maximum in this sample). The occurrence of *Camerosporites seccatus* above this hiatus indicates still a Carnian age (Kurschner and Herngreen, 2010). The duration of this hiatus is unknown.

Assemblage B_2 although is mudstone-dominated, consists of varied lithology including red, green, grey, dark mudstones and thin breccia layers. The highest relevant abundance is that of charcoal regarding the palynofacies trends and the pollen/spores variety is relatively low. Those two factors coupled together reveal that the climatic conditions at the time were less favourable for vegetation to thrive. In addition to this, the samples are plotted away from the 'terrestrial palynomorphs' corner in the ternary plot supporting the view of low variety of pollen/spores (fig. 18). The high relevant abundance values of charcoal may very well document a transition to a hotter and drier climate. The clay mineral analysis indicates the presence of sylvite (sample WE214) and absence of kaolinite. Smectite is present only in sample WE206, above from which there is no sufficient sampling. The total lack of kaolinite together with the -almost complete- absence of smectite, imply that the climate became less wet and probably hotter compared to B_1. Moreover, the optical microscopy (samples WE215 and WE206) denied the presence of any kind of ooids.

The depositional environment in B_2 appears to be between marginal lacustrine, and more distal from the lake system, if there was any at all. The results presented here suggest a period during which, the evaporation was more dominant than precipitation and weathering, as manifested by the high proportions of red mudstones, the low variety of palynoflora, the high relevant abundances of charcoal, the absence of kaolinite and the presence of sylvite and hematite.

The dense sampling terminates at sample WE204. On the uppermost part of the section where samples WE203 and WE202 are located, there are some indications of a shift towards a wetter climate again, but the lack of additional samples restrains the ability to make any kind of accurate conclusion.

Comparison with other studies and synopsis

The interpretation of the depositional environments in the present study, come in great correspondence with those of previous studies (Gallois and Porter, 2008, Porter and Gallois, 2006, Milroy and Wright, 2000, Milroy and Wright, 2002). Jeans (1978 and 2006) suggests the clay mineral assemblages are influenced by marine incursions resulting temporarily in hypersaline conditions and he believes this varies laterally. In the present study no evidence for marine influence has been retrieved; quite the opposite has been concluded, especially taking into account the thriving of the fresh-water alga *Plaesiodictyon* which is also known to have the ability to spread by aerobiological methods (Zavattieri and Mercedes, 2006). The peak of the humidification of the climate in the studied section is most likely expressed in the interval covered by the assemblage A_3. This is documented by the dominance of dolomitic layers, the thriving of *Plaeisiodictyon* (oxygenated waters and probably higher energy) and vegetation manifested by the high variety of pollen/spores, the presence of kaolinite (sample WE015), the presence of big-sized ooids and the coarser grained nature.

6. Conclusions

From this work the following conclusions can be made:

1) Presence of the species *Camerosporites seccatus* indicates a Carnian age for the section.
2) The lithological variations of the studied section appear to be connected to the palaeoclimate pattern and the characteristics of the interval covered by assemblage A_3 match well those of the Julian humid pulse as suggested by previous studies.
3) The depositional environments encountered are mostly lacustrine and range from fluvial/lacustrine to marginal lacustrine and fresh-water lake/lacustrine. No indications of marine influence have been found.
4) The palynofacies analysis seems to be an efficient tool for correlation with sedimentology. Additional work could reveal more interesting results. For example, counting the *Lycopodium* spore for each sample can provide information about the sedimentation rates. This information can be linked to the palaeomagnetic data and unfold more accurately the time span of the studied section. By achieving this, it might become possible to go further in determining if the causes are associated with the Milankovitch cycles, the regional tectonic framework etc.
5) The clay mineral analysis determining the kaolinite (both qualitatively and quantitatively) and smectite (qualitatively) managed to give information as palaeoclimatic indicators. Extra detailed work on defining which smectite and illite minerals are involved precisely and in what quantities, will definitely give even better resolution.
6) The common occurrence of smectite in some parts of the section is well explained by the low relief and ties with references from previous works.

7. Appendix

Taxonomy

Spores

Genus *Calamospora* Schopf, Wilson & Bentall, 1944

Calamospora sp.

Trilete spore with oval to rounded shape. It usually bears a characteristic triradiate tetrad mark. It has a very thin, smooth exine that sometimes makes the specimens transparent.

Genus *Porcellispora* Scheuring, 1970

Porcellispora sp.

Spore with circular to oval shape. Its main characteristics are the sponge-like texture of the exine (punctate) and the fact that it is double walled.

Pollen

Genus *Camerosporites* Leschik, 1956 emended

Camerosporites seccatus Leschik, 1956 emended

Multisculptured trilete spore with a curvature perfecta, which means it has three lines complete all around the proximal face. The ornamentation was difficult to. In literature where SEM/TEM was used, it is referred to have verrucae, microrugulae and occasional gemmae (Litwin and Skog, 1991).

This pollen has circular shape with a circular cryptospore on the distal pole. On the proximal pole a triangular scar with concave sides can be seen. Subequatorially there is a circular groove parallel to the equator of the grain. The exine seems smooth, but it might be needed SEM to able to define it with certainty.

Remarks (Kurschner and Herngreen, 2010): Indicator of Carnian age.

Genus *Duplicisporites* (Potonie, 1931, Leschik, 1955) Klaus, 1960

Duplicisporites sp.

This grain has subcircular shape, granular ornamentation on the exine and three distinct folds on the distal side. Its most profound feature is its triletes scar which looks like a triangle is clearly visible on all specimens.

Genus *Enzonalasporites* Leschik, 1955

Enzonalasporites sp.

On the equatorial view this grain has circular shape. The exine ornamentation consists of-not so closely- spaced spines and it has a groove that extends from one side to the other.

Genus *Ovalipollis* Krutzsch, 1955 emend. Pocock & Jansonius

Ovalipollis sp. *A*

A bisaccate pollen with narrow shaped air-sacs as seen on the equatorial view. Its shape is ellipticial and there is a longitudinal, thin furrow (more like slit) which looks as if it splits the pollen into two symmetrical parts. The ornamentation is complicated and alternates between punctate, rugulate and reticulate, usually with gradual transition.

Ovalipollis sp. *B*

This species shows similar characteristics to *Ovalipollis* sp. *A*, with two main differences. First, the air-sacs have a spinule structure which gives them a different, darker look and second, the longitudinal furrow is thicker. In terms of size, this species is slightly smaller in length.

Genus *Praecirculina* Klaus, 1960

Praecirculina sp.

This pollen grain on the equatorial view has a characteristic incomplete, semicircular furrow. Sometimes a trilete mark can be seen and often looks like it has structure like double-walled. It can sometimes be confused with *Corollina sp.* because both of them seem to have smooth surface.

Genus *Triadispora* Klaus, 1964

Triadispora sp.

A bisaccate pollen that is possible to be distinguished from the rest of the bisaccates as it often carries a trilete mark (three laesurae) on the main body or some other irregular laesurae structures which may probably vary among the different forms (or species). The equatorial view is usually circular or slightly oval shaped.

Algae

Division CHLOROPHYTA Pascher, 1914

Class CHLOROPHYCEAE Kützing, 1843

Order CHLOROCOCCALES Marchand, 1895

Family HYDRODICTYACEAE (Gray) Dumortier, 1829

Genus PLAESIODICTYON Wille, 1970

Plaesiodictyon sp.

Plaesiodictyon is a fossil -only- genus of colonial chlorococcalean algae recorded so far only in Triassic sediments (Zavattieri, 2006; Wood and Benson, 2010). Its characteristic geometry looks like a net style structure consisting of cells arranged in quadrangular planar coenobia. The identification is hard to be done in species level although there is a possibility two separate species might be present. In some forms, the skeleton of this net-like structure appears to be thicker than others. In these forms, there also seems to be continuous, connective tissue all over the specimen. In contrast, some other forms appear with a significantly thinner skeleton and have gaps in the quadrangular planar coenobia (Pl.1, fig.3 top left). The criteria are poor hence they are all included under one category.

Remarks (from Zavattieri, 2006): This freshwater alga has been profoundly discussed not only about its palaeoecological and palaeoenvironmental implications, but also because of its palaeogeographical and biostratigraphic significance. In many occasions it can be used effectively to correlate between different locations. Aerobiological methods have been proposed to explain why this genus has been dispersed very quickly in a quite short amount of geological time.

Family BOTRYOCOCCACEAE Wille, 1909

Genus BOTRYOCOCCUS Kützing, 1849

Botryococcus sp.

Botryococcus is a monadic self-supported colonial alga with an appearance very similar to a string of grapes. It is very hard to divide into species and in my samples many times the preservation is so poor that it is included in the ‘AOM’ category.

Remarks (from Ji et al., 2010): Present day *Botryococcus* lives in terrestrial regions in fresh to brackish water lakes and seawater in estuaries in temperate and tropical climates. It requires sufficient sunlight, calm and clear water. In Mesozoic times it was found in limnetic lacustrine sediments.

Tables and Plates

Table 1: Palynofacies countings.

Sample no.	*m above base*	AOM	Charcoal	Wood fragments	Cuticle fragments	Plant tissue	Pollen/Spores	Algae	Total
WE 304	4	0	30	0	0	17	13	240	300
WE 001	9,6	37	164	15	0	24	50	10	300
WE 002	10,4	5	274	4	0	0	2	15	300
WE 003	12,1	4	55	13	0	5	223	0	300
WE 004	12,8	37	153	19	0	36	38	100	383
WE 005	13,2	4	282	12	0	9	28	3	338
WE 006	14,4	202	17	1	0	0	1	79	300
WE 007	15,5	244	14	0	0	5	7	30	300
WE 008	16,1	15	251	20	0	12	4	3	305
WE 009	17,1	141	52	9	0	28	60	10	300
WE 011	17,7	70	81	5	0	14	119	11	300
WE 012	17,9	104	80	15	0	15	50	36	300
WE 014	19,9	5	19	3	0	9	18	255	309
WE 015	20,4	55	15	2	0	4	230	0	306
WE 016	20,6	180	85	23	0	0	4	15	307
WE 017	21,5	1	19	2	2	11	75	190	300
WE 018	22,4	3	45	6	0	4	14	230	302
WE 019	22,6	6	71	3	14	22	17	175	308
WE 115	25,4	3	15	0	6	10	2	274	310
WE 108	29,6	195	9	1	0	14	24	121	364

WE 109	30,1	37	212	5	1	14	45	5	319
WE 111	30,5	130	73	8	0	19	33	37	300
WE 110	30,9	175	55	0	0	0	90	0	320
WE 103	31,1	116	35	13	0	2	162	0	328
WE 104	31,5	37	80	3	4	13	151	12	300
WE 112	32,4	26	86	5	8	59	79	37	300
WE 301	33,3	210	90	0	0	0	0	0	300
WE 305	34,8	145	17	11	0	5	118	4	300
WE 302	35,5	70	28	2	0	0	200	0	300
WE 303	36,5	135	85	2	1	3	64	26	316
WE 216	39,4	10	274	5	1	5	0	5	300
WE 214	41,6	38	73	17	7	38	47	80	300
WE 213	42,6	33	300	22	0	3	9	6	373
WE 212	43,3	18	165	21	0	2	28	114	348
WE 209	43,8	104	89	2	0	30	41	34	300
WE 208	45,2	105	22	1	0	6	20	146	300
WE 206	45,6	115	122	13	0	7	5	63	325
WE 203	53	0	31	12	0	1	180	90	314

Table 2: Palynological sample correlation between Fisher (1985) and this study.

My samples	Fisher (1985)
WE003	De165
WE009	De242
WE011	De292
WE015	De241
WE017	De240 De168 De169
WE018	De163
WE019	De170
WE106	De81
WE111	De152
WE110	De150
WE103	De76
WE104	De77
WE301	De78
WE214	De69
WE213	De67

Table 3: The mineral phases and their main identification peaks.

Minerals	**d values (Å)**
Dolomite/Ankerite	~2.89
Calcite	~3
Quartz	~3.34
Kaolinite	~7
Chlorite/Smectite	~7, 14
Illite	~10
K-feldspar	~3.21, 3.24, 3.29-3.31
Sepiolite	~12
Hematite	~2.70
Sylvite	~3.14
Pyrite	~2.71

Plate 1

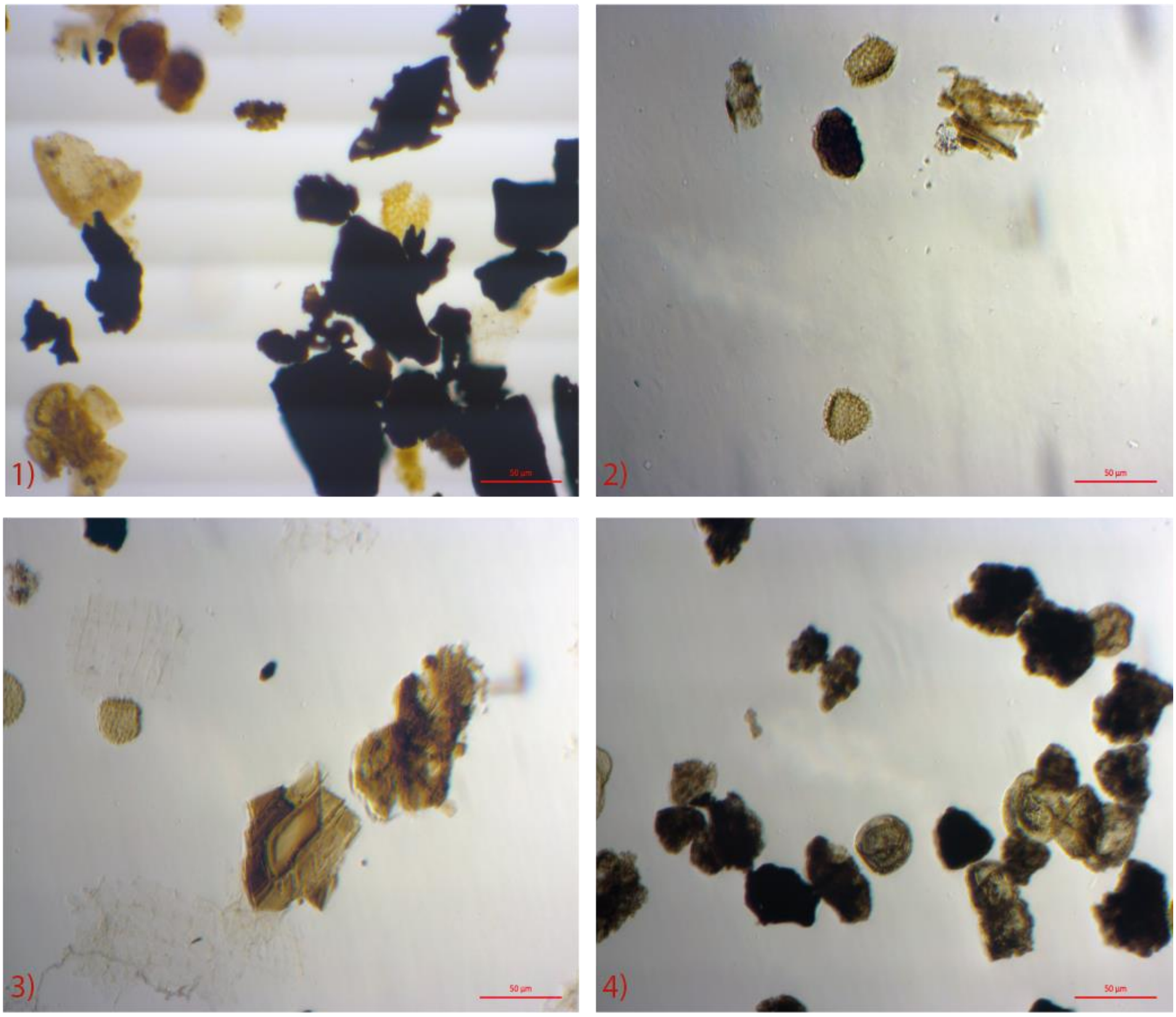

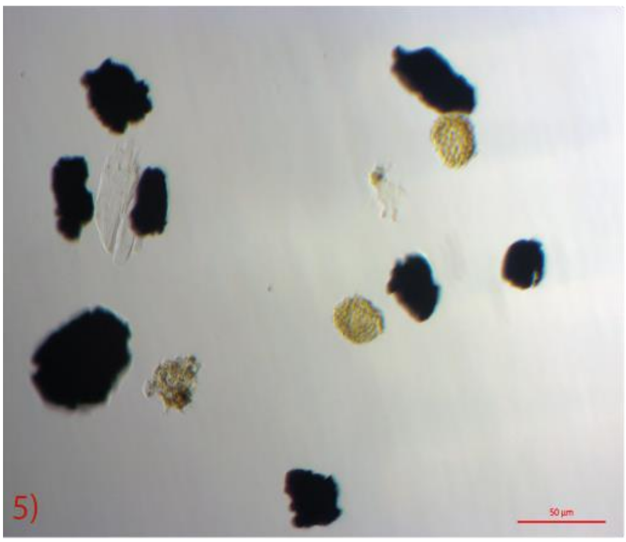

Plate 1: Examples of palynofacies assemblages. 1) Assemblage A1: Predominantly charcoal, a pollen tetrad, plant fragments and *Botryococcus*. 2) Assemblage A2: Charcoal, plant tissue, *Lycopodium*, AOM. Not dense slide. 3) Assemblage A3: *Plaesiodictyon*, plant tissue, *Lycopodium*, charcoal. 4) Assemblage B1: AOM, pollen and spores, charcoal. Scarce *Lycopodium*. 5) Assemblage B2:

Plate 2

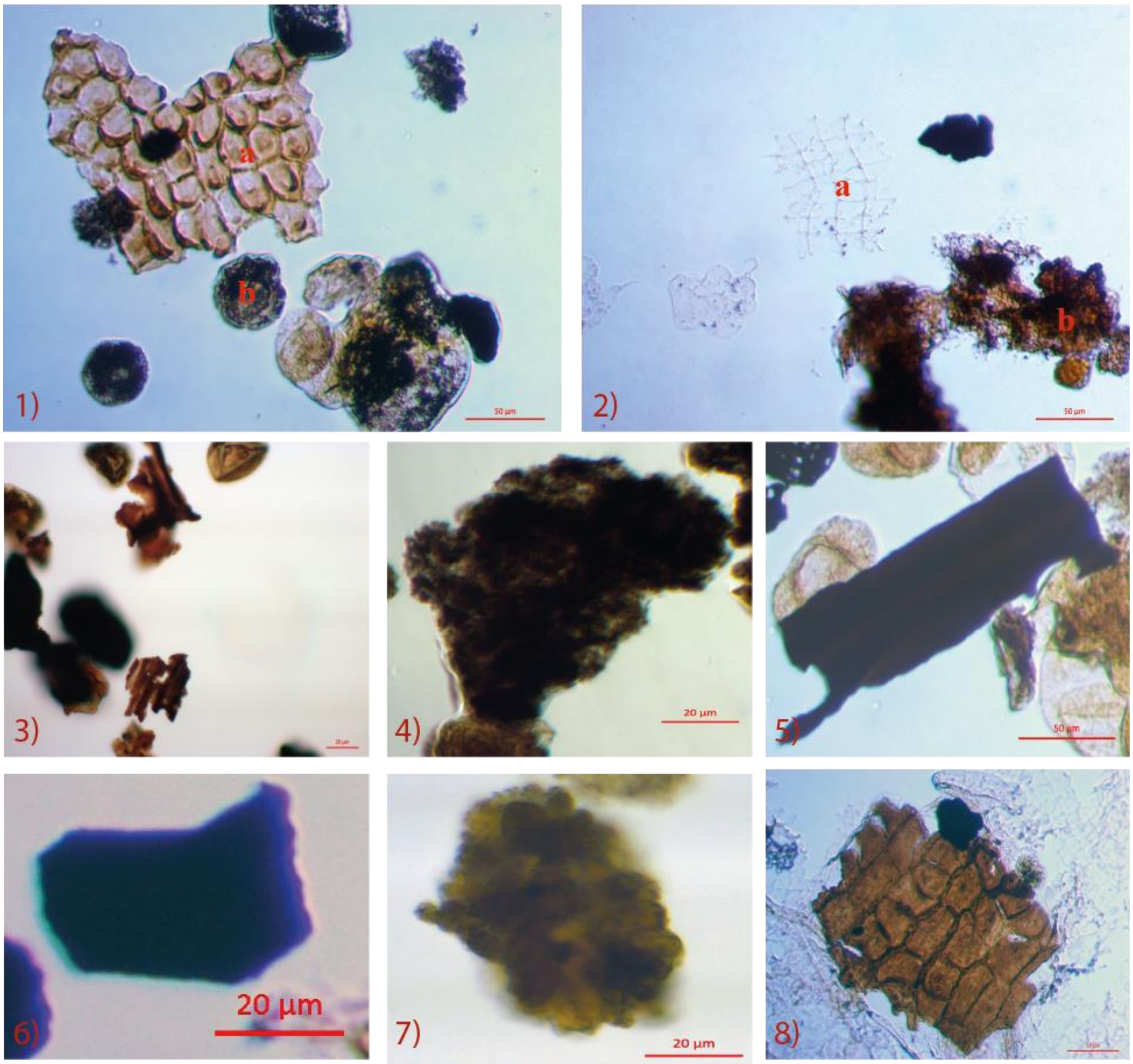

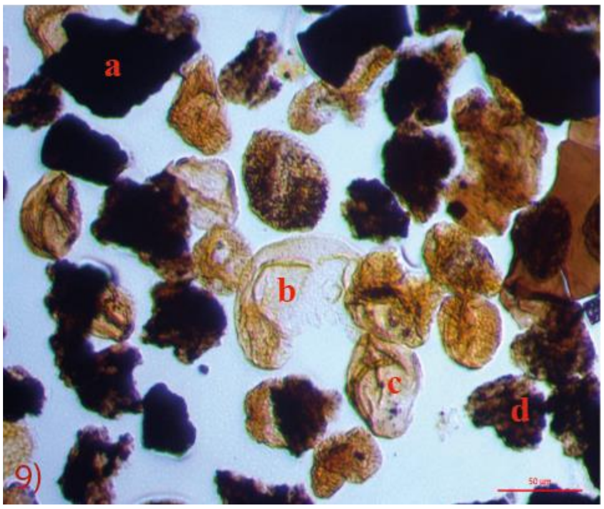

Plate 2: Examples of OM encountered in the slides. 1) a: Cuticle fragment. b: Pollen. 2) a: *Plaesiodictyon* sp. b: *Botryococcus* sp. 3) Plant fragments, 4) AOM, 5) Wood fragment, 6) Charcoal. 7) *Botryococcus* sp. 8) Cuticle fragment. 9) a: Charcoal, b) Bisaccate pollen, c) Spore, d) AOM.

Plate 3

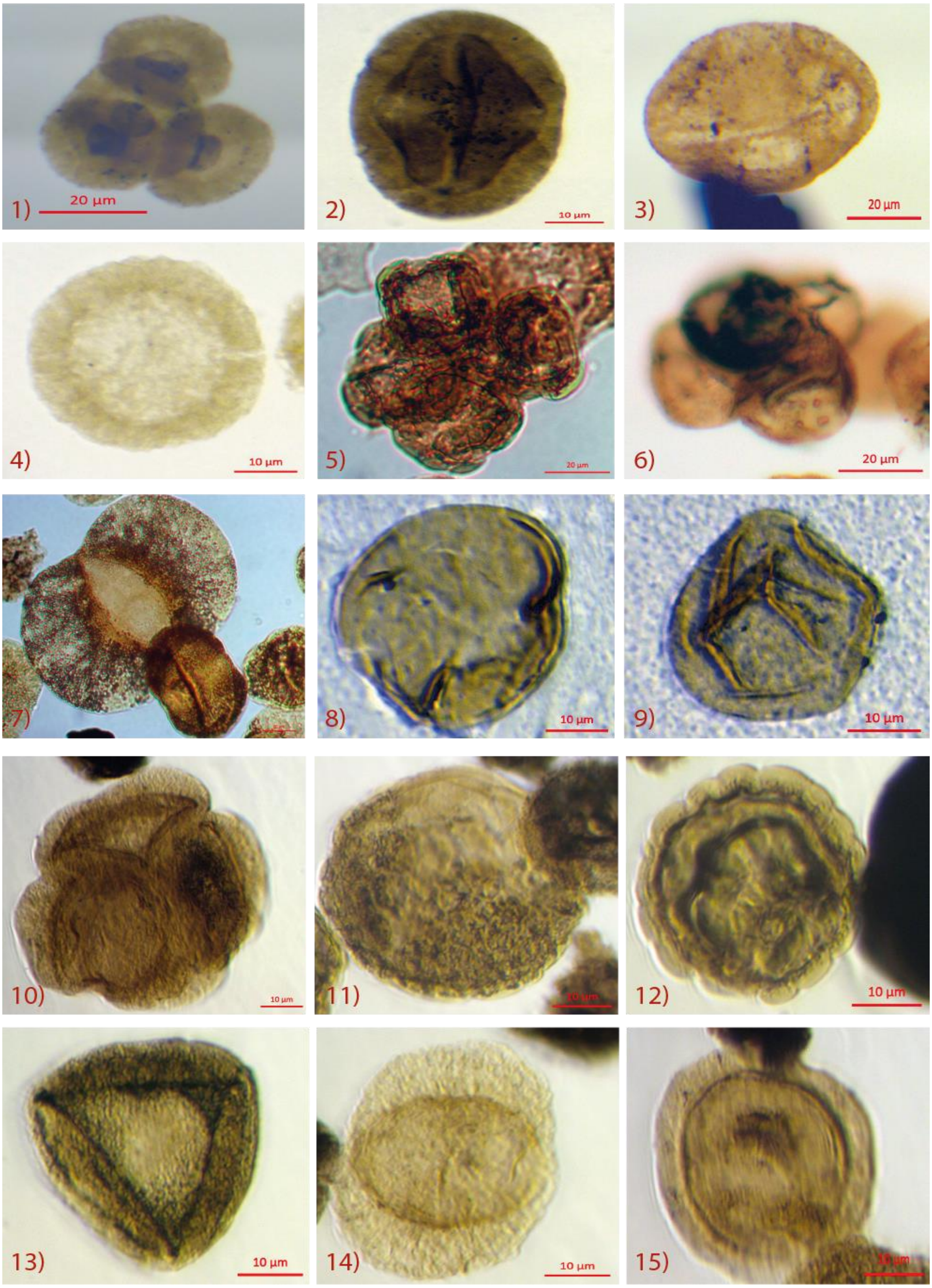
1) 20 µm
2) 10 µm
3) 20 µm
4) 10 µm
5) 20 µm
6) 20 µm
7)
8) 10 µm
9) 10 µm
10) 10 µm
11)
12) 10 µm
13) 10 µm
14) 10 µm
15) 10 µm

Plate 3: 1) Camersporites tetrad. 2) Ovalipollis sp. 2. 3) Ovalipollis sp.1. 4) Enzonalasporites sp. 5) Camerosporites tetrad. 6) Praecirculina tetrad. 7) a) Bisaccate, b) Ovalipollis sp. 1. 8) Praecirculina sp. 9) Calamospora sp. 10) Bisaccate tetrad. 11) Porcellispora sp. 12) Camersporites sp. cf. seccatus. 13) Duplicisporites sp. 14) Triadispora sp. 15) Enzonalasporites sp.

Plate 4

WE303 (Coupled TwoTheta/Theta)

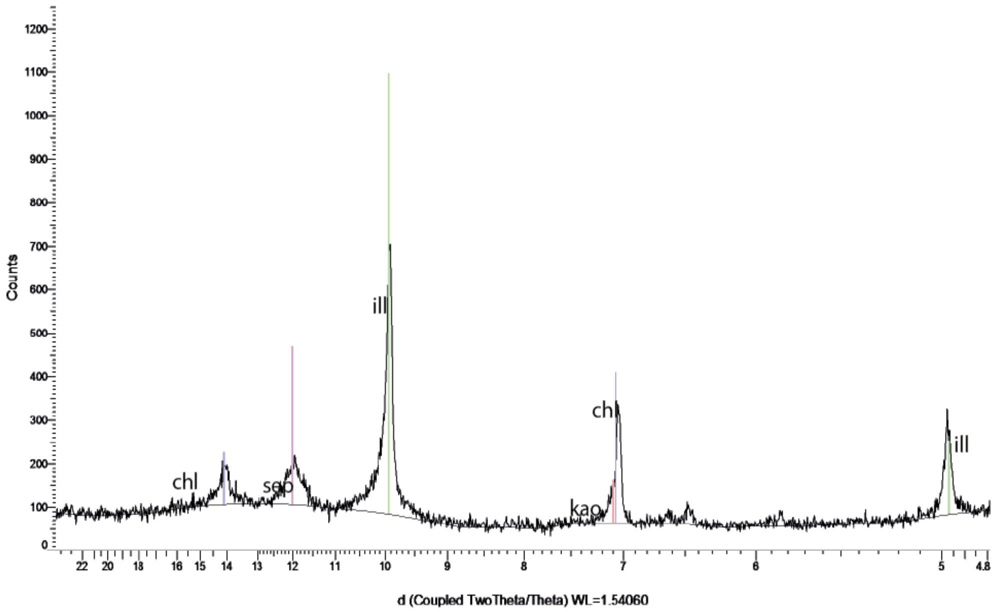

WE009 (Coupled TwoTheta/Theta)

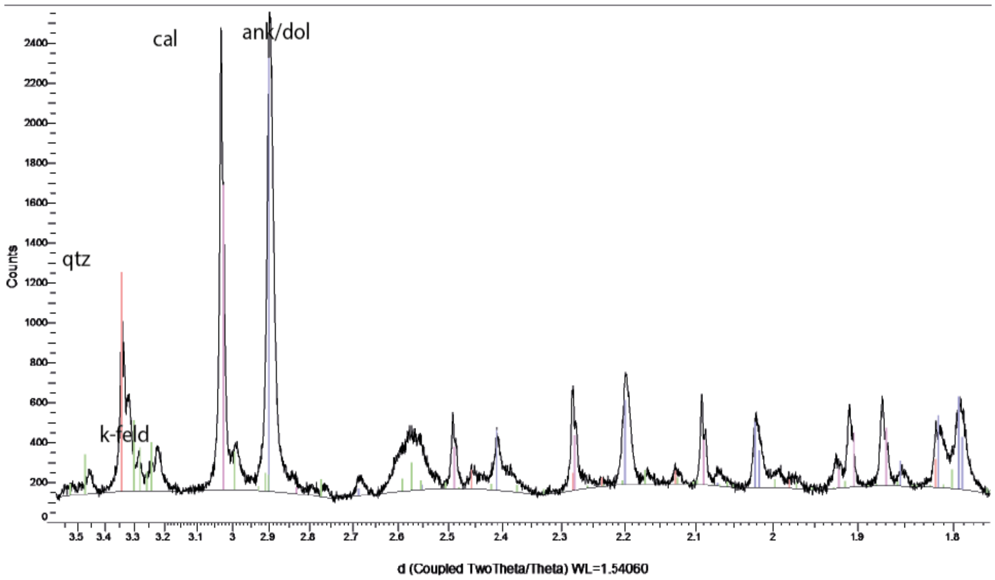

Plate 5

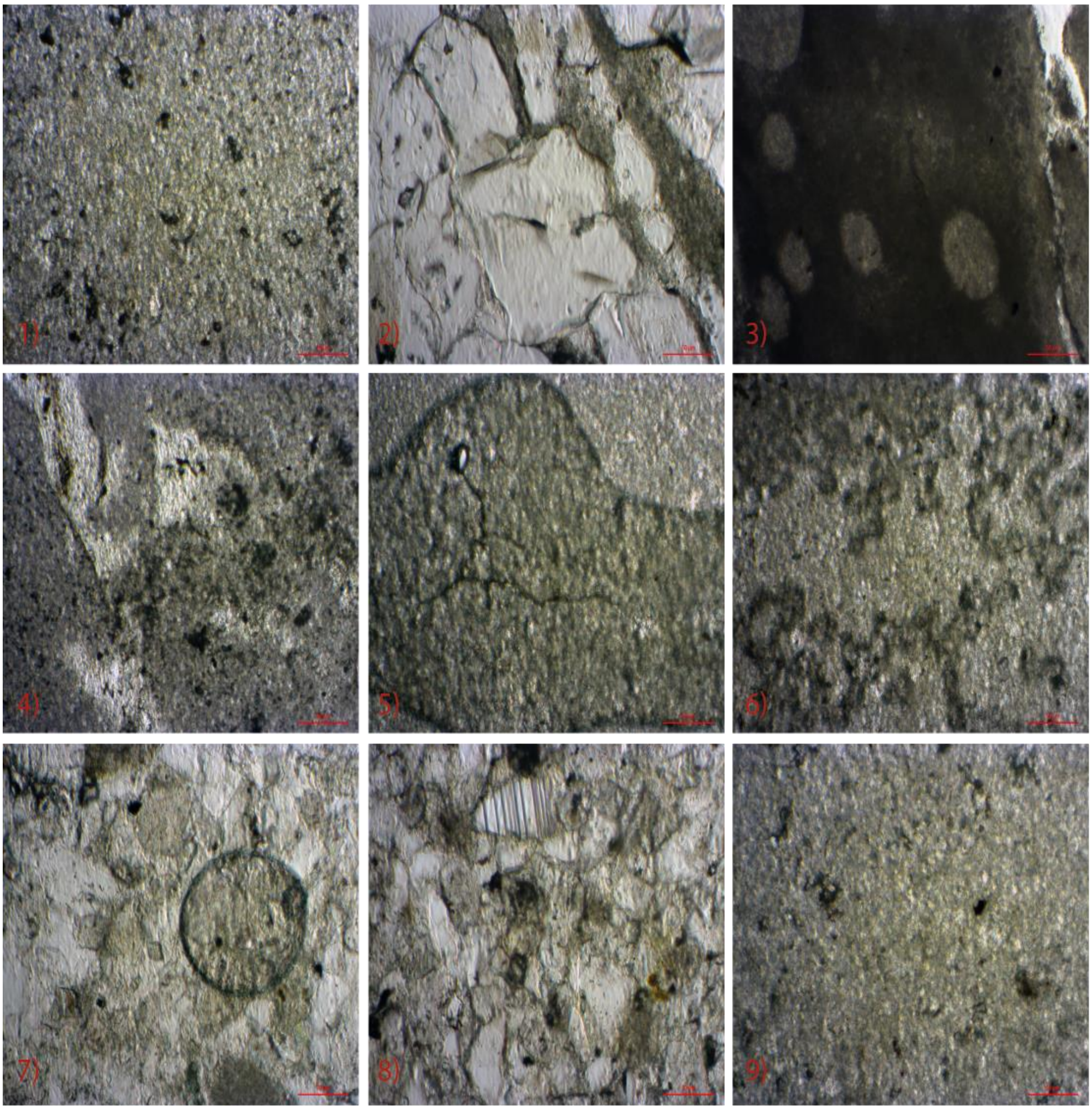

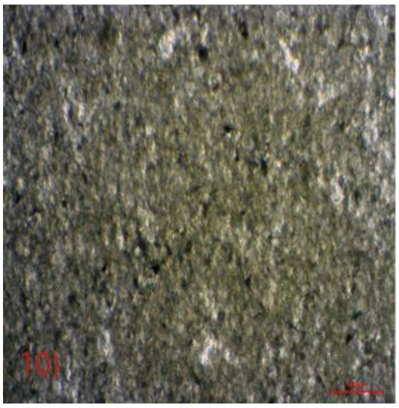

Plate 5: The thin sections under the microscope: 1) Sample WE011, mainly micritic material and some dark grains. 2) Sample WE011, sparitic and micritic material. 3) Sample WE011, ooids in micritic material. 4) Sample WE012, micritic material and some sparitic. 5) Sample WE012b, T5 grain. 6) Sample WE012b, T5 grain texture with micritic material. 7) Sample WE101, T6 grains, sparitic material, big sized ooids. 8) Sample WE202, sparitic, very few ooids, calcite. 9) Sample WE206, micritic material with dark grains. 10) Sample WE215, micritic material with dark grains.

8. References

Arche, A., and López-Gómez, J., 2014, The Carnian Pluvial Event in Western Europe: New data from Iberia and correlation with the Western Neotethys and Eastern North America–NW Africa regions: Earth-Science Reviews, v. 128, p. 196-231.

Bonis, N. R., Ruhl, M., and Kürschner, W. M., 2010, Climate change driven black shale deposition during the end-Triassic in the western Tethys: Palaeogeography, Palaeoclimatology, Palaeoecology, v. 290, no. 1–4, p. 151-159.

Dal Corso, J., Gianolla, P., Newton, R. J., Franceschi, M., Roghi, G., Caggiati, M., Raucsik, B., Budai, T., Haas, J., and Preto, N., 2015, Carbon isotope records reveal synchronicity between carbon cycle perturbation and the "Carnian Pluvial Event" in the Tethys realm (Late Triassic): Global and Planetary Change, v. 127, no. 0, p. 79-90.

Dal Corso, J., Mietto, P., Newton, R. J., Pancost, R. D., Preto, N., Roghi, G., and Wignall, P. B., 2012, Discovery of a major negative δ13C spike in the Carnian (Late Triassic) linked to the eruption of Wrangellia flood basalts: Geology, v. 40, no. 1, p. 79-82.

Dickins, J. M., 1993, Climate of the Late Devonian to Triassic: Palaeogeography, Palaeoclimatology, Palaeoecology, v. 100, no. 1–2, p. 89-94.

Doré, A. G., 1992, Synoptic palaeogeography of the Northeast Atlantic Seaway: late Permian to Cretaceous: Geological Society, London, Special Publications, v. 62, no. 1, p. 421-446.

Fisher, M., 1985, Palynology of sedimentary cycles in the Mercia mudstone and Penarth group (Triassic) of southwest and central England: Pollen et spores, v. 27, no. 1, p. 95-112.

Fisher, M. J., 1972, The Triassic palynofloral succession in England: Geoscience and Man, v. 4, no. 1, p. 101-109.

Fisher, M. J. J., C. V., 1982, Clay mineral stratigraphy in the Permo-Triassic red bed sequences of BNOC 72/10-1A, Western Approaches, and the south Devon coast: Clay Minerals, v. 17, p. 79-89.

Gallois, R. W., 2001, The stratigraphy of the Mercia Mudstone Group (Mid to Late Triassic) of the south Devon coast: Geoscience in south-west England, v. 10, p. 195-204.

-, 2007, The stratigraphy of the Mercia Mudstone Group succession (Mid to Late Triassic) proved in the Wiscombe Park boreholes, Devon: Geoscience in south-west England, v. 11, p. 280-286.

Gallois, R. W., and Porter, R. J., 2006, The stratigraphy and sedimentology of the Dunscombe Mudstone Formation (Late Triassic) of south-west England: Geoscience in south-west England, v. 11, p. 174-182.

Haas, J., Budai, T., and Raucsik, B., 2012, Climatic controls on sedimentary environments in the Triassic of the Transdanubian Range (Western Hungary): Palaeogeography, Palaeoclimatology, Palaeoecology, v. 353-355, p. 31-44.

Hallam, A., 1985, A review of Mesozoic climates: Journal of the Geological Society, v. 142, no. 3, p. 433-445.

Hochuli, P. A., and Vigran, J. O., 2010, Climate variations in the Boreal Triassic — Inferred from palynological records from the Barents Sea: Palaeogeography, Palaeoclimatology, Palaeoecology, v. 290, no. 1–4, p. 20-42.

Hornung, T., and Brandner, R., 2005, Biochronostratigraphy of the Reingraben Turnover (Hallstatt Facies Belt): Local black shale events controlled by regional tectonics, climatic change and plate tectonics: Facies, v. 51, no. 1-4, p. 460-479.

Hornung, T., Krystyn, L., and Brandner, R., 2007a, A Tethys-wide mid-Carnian (Upper Triassic) carbonate productivity crisis: Evidence for the Alpine Reingraben Event from Spiti (Indian Himalaya)?: Journal of Asian Earth Sciences, v. 30, no. 2, p. 285-302.

Hornung, T. B., R., Krystyn, L. J., M. M., and Keim, L., 2007b, Multistratigraphic constraints on the NW Tethyan 'Carnian Crisis', New Mexico Museum of Natural History and Science Bulletin, The Global Triassic.

Hounslow, M. M., G., Gallois, R. W., and Jenkins, G., 2002, Anisian, Ladinian and Carnian non-marine magnetostratigraphic reference section: the coastal exposures between Budleigh Salterton and Branscombe, South Devon, U.K.: Geoscience in south-west England, v. 10.

Howard, A. S. W., G., Ambrose, K., and Rees, J. G., 2008, A formational framework for the Mercia Mudstone Group (Triassic) of England and Wales.

Jeans, C. V., 1978, The Origin of the Triassic Clay Assemblages of Europe with Special Reference to the Keuper Marl and Rhaetic of Parts of England, v. 1365, 549-636 p.:

Ji, L.-m., Yan, K., Meng, F.-w., and Zhao, M., 2010, The oleaginous Botryococcus from the Triassic Yanchang Formation in Ordos Basin, Northwestern China: Morphology and its paleoenvironmental significance: Journal of Asian Earth Sciences, v. 38, no. 5, p. 175-185.

Kolar-Jurkovšek, T., and Jurkovšek, B., 2010, New paleontological evidence of the Carnian strata in the Mežica area (Karavanke Mts, Slovenia): Conodont data for the Carnian Pluvial Event: Palaeogeography, Palaeoclimatology, Palaeoecology, v. 290, no. 1-4, p. 81-88.

Kozur, H. W., and Bachmann, G. H., 2010, The Middle Carnian Wet Intermezzo of the Stuttgart Formation (Schilfsandstein), Germanic Basin: Palaeogeography, Palaeoclimatology, Palaeoecology, v. 290, no. 1-4, p. 107-119.

Kuerschner, W. M., Bonis, N. R., and Krystyn, L., 2007, Carbon-isotope stratigraphy and palynostratigraphy of the Triassic–Jurassic transition in the Tiefengraben section — Northern Calcareous Alps (Austria): Palaeogeography, Palaeoclimatology, Palaeoecology, v. 244, no. 1–4, p. 257-280.

Kurschner, W. M., and Herngreen, G. F. W., 2010, Triassic palynology of central and northwestern Europe: a review of palynofloral diversity patterns and biostratigraphic subdivisions: Geological Society, London, Special Publications, v. 334, no. 1, p. 263-283.

Leslie, A. B., and Spiro, B. T., M. E., 1993, Geochemical and mineralogical variations in the upper Mercia Mudstone Group (Late Triassic), southwest Britain: correlation of outcrop sequences with borehole geophysical logs: Journal of the Geological Society, London, v. 150, p. 67-75.

Litwin, R. J., and Skog, J. E., 1991, Morphology and palynostratigraphy of the genus Camerosporites Leschik 1956: Palynology, v. 15, no. 1, p. 5-28.

McKie, T., and Williams, B., 2009, Triassic palaeogeography and fluvial dispersal across the northwest European Basins: Geological Journal, v. 44, no. 6, p. 711-741.

Milroy, P., and Wright, V., 2002, Fabrics, facies control and diagenesis of lacustrine ooids and associated grains from the Upper Triassic, southwest England: Geological Journal, v. 37, no. 1, p. 35-53.

Milroy, P. G., and Wright, V. P., 2000, A highstand oolitic sequence and associated facies from a Late Triassic lake basin, south-west England: Sedimentology, v. 47, no. 1, p. 187-209.

Moore, D. M., and Reynolds, R. C., 1989, X-ray Diffraction and the Identification and Analysis of Clay Minerals, Oxford university press Oxford.

Mueller, S., Krystyn, L., and Kürschner, W. M., 2015, Climate variability during the Carnian Pluvial Phase — A quantitative palynological study of the Carnian sedimentary succession at Lunz am See, Northern Calcareous Alps, Austria: Palaeogeography, Palaeoclimatology, Palaeoecology.

Mueller, S., Veld, H., Nagy, J., and Kürschner, W. M., 2014, Depositional history of the Upper Triassic Kapp Toscana Group on Svalbard, Norway, inferred from palynofacies analysis and organic geochemistry: Sedimentary Geology, v. 310, p. 16-29.

Ogg, J., 2015, The mysterious Mid-Carnian “Wet Intermezzo” global event: Journal of Earth Science, v. 26, no. 2, p. 181-191.

Porter, R. J., and Gallois, R. W., 2008, Identifying fluvio–lacustrine intervals in thick playa-lake successions: An integrated sedimentology and ichnology of arenaceous members in the mid–late Triassic Mercia Mudstone Group of south-west England, UK: Palaeogeography, Palaeoclimatology, Palaeoecology, v. 270, no. 3-4, p. 381-398.

Preto, N., Kustatscher, E., and Wignall, P. B., 2010, Triassic climates — State of the art and perspectives: Palaeogeography, Palaeoclimatology, Palaeoecology, v. 290, no. 1-4, p. 1-10.

Retallack, G. J., Veevers, J. J., and Morante, R., 1996, Global coal gap between Permian–Triassic extinction and Middle Triassic recovery of peat-forming plants: Geological Society of America Bulletin, v. 108, no. 2, p. 195-207.

Rigo, M., Preto, N., Roghi, G., Tateo, F., and Mietto, P., 2007, A rise in the Carbonate Compensation Depth of western Tethys in the Carnian (Late Triassic): Deep-water evidence for the Carnian Pluvial Event: Palaeogeography, Palaeoclimatology, Palaeoecology, v. 246, no. 2-4, p. 188-205.

Roghi, G., Gianolla, P., Minarelli, L., Pilati, C., and Preto, N., 2010, Palynological correlation of Carnian humid pulses throughout western Tethys: Palaeogeography, Palaeoclimatology, Palaeoecology, v. 290, no. 1-4, p. 89-106.

Rostási, Á., Raucsik, B., and Varga, A., 2011, Palaeoenvironmental controls on the clay mineralogy of Carnian sections from the Transdanubian Range (Hungary): Palaeogeography, Palaeoclimatology, Palaeoecology, v. 300, no. 1-4, p. 101-112.

Ruffell, A. H., and Hounslow, M., 2006, Triassic: seasonal rivers, dusty deserts and saline lakes, Geological Society of London, The Geology of England & Wales.

Sebag, D., Copard, Y., Di-Giovanni, C., Durand, A., Laignel, B., Ogier, S., and Lallier-Verges, E., 2006, Palynofacies as useful tool to study origins and transfers of particulate organic matter in recent terrestrial environments: Synopsis and prospects: Earth-Science Reviews, v. 79, no. 3-4, p. 241-259.

Simms, M. J., and Ruffell, A. H., 1989, Synchroneity of climatic change and extinctions in the Late Triassic: Geology, v. 17, no. 3, p. 265.

Traverse, A., 2007, Paleopalynology, second edition, Springer, Topics in Geobiology.

Tyson, R., 2012, Sedimentary organic matter: organic facies and palynofacies, Springer Science & Business Media.

Visscher, H., Van Houte, M., Brugman, W. A., and Poort, R. J., 1994, Rejection of a Carnian (Late Triassic) 'pluvial event' in Europe: Review of Palaeobotany and Palynology, v. 83, p. 217-226.

Warrington, G., 1970, The stratigraphy and palaeontology of the'Keuper'Series of the central Midlands of England: Quarterly Journal of the Geological Society, v. 126, no. 1-4, p. 183-223.

Wilson, M., 2013, Sheet Silicates: Clay Minerals, Geological Society.

Wood, G. D., and Benson, D. G., 2010, The north american occurrence of the algal coenobiumplaesiodictyon'.paleogeographic, paleoecologic, and biostratigraphic importance in the Triassic: Palynology, v. 24, no. 1, p. 9-20.

Zavattieri, A. M. P., Mercedes B., 2006, Freshwater algae from the Upper Triassic Cuyana basin of Argentina: Palaeoenvironmental implications: Paleontology, v. 49, p. 1185-1209.